



1 **The Interactive Stratospheric Aerosol Model Intercomparison**

2 **Project (ISA-MIP): Motivation and experimental design**

3 Claudia Timmreck¹, Graham W. Mann^{2,3}, Valentina Aquila⁴, Rene Hommel^{5,*} Lindsay A.
4 Lee², Anja Schmidt^{6,7}, Christoph Brühl⁸, Simon Carn⁹, Mian Chin¹⁰, Sandip S. Dhomse²,
5 Thomas Diehl¹¹, Jason M. English^{12,13}, Michael J. Mills¹⁴, Ryan Neely^{2,3}, Jianxiong
6 Sheng^{15,16}, Matthew Toohey^{1,17}, and Debra Weisenstein¹⁶

7 ¹Max-Planck-Institute for Meteorology, Hamburg, Germany

8 ²School of Earth and Environment, University of Leeds, Leeds, UK

9 ³UK National Centre for Atmospheric Science, University of Leeds, Leeds, UK

10 ⁴American University, Dept. of Environmental Science Washington, DC, USA

11 ⁵Institute of Environmental Physics, University of Bremen, Bremen, Germany

12 ⁶Department of Chemistry, University of Cambridge, Lensfield Road, Cambridge CB2 1EW, UK

13 ⁷Department of Geography, University of Cambridge, Downing Place, Cambridge CB2 3EN, UK

14 ⁸Max-Planck-Institute for Chemistry, Mainz, Germany

15 ⁹Dept Geo Min Eng Sci MTU, Houghton, MI, USA

16 ¹⁰NASA Goddard Space Flight Center, Greenbelt, MD 20771, USA

17 ¹¹Directorate for Sustainable Resources, Joint Research Centre, European Commission, Ispra, Italy

18 ¹²University of Colorado, Cooperative Institute for Research in Environmental Sciences

19 ¹³NOAA Earth Systems Laboratory, Boulder, CO, USA

20 ¹⁴Atmospheric Chemistry Observations and Modeling, National Center for Atmospheric Research, Boulder, CO,
21 USA

22 ¹⁵ETHZ, Zürich, Switzerland

23 ¹⁶John A. Paulson School of Engineering and Applied Sciences, Harvard University, Cambridge, MA, USA

24 ¹⁷GEOMAR Helmholtz Centre for Ocean Research, Kiel, Germany

25 * now at Hommel & Graf Environmental, Hamburg, Göttingen, Germany

26 *Correspondence to:* Claudia Timmreck (claudia.timmreck@mpimet.mpg.de)

27 **Abstract** The Stratospheric Sulfur and its Role in Climate (SSiRC) interactive stratospheric aerosol model
28 intercomparison project (ISA-MIP) explores uncertainties in the processes that connect volcanic emission of
29 sulphur gas species and the radiative forcing associated with the resulting enhancement of the stratospheric
30 aerosol layer. The central aim of ISA-MIP is to constrain and improve interactive stratospheric aerosol models
31 and reduce uncertainties in the stratospheric aerosol forcing by comparing results of standardized model
32 experiments with a range of observations. In this paper we present 4 co-ordinated inter-model experiments
33 designed to investigate key processes which influence the formation and temporal development of stratospheric
34 aerosol in different time periods of the observational record. The “Background” (BG) experiment will focus on
35 microphysics and transport processes under volcanically quiescent conditions, when the stratospheric aerosol is
36 controlled by the transport of aerosols and their precursors from the troposphere to the stratosphere. The
37 “Transient Aerosol Record” (TAR) experiment will explore the role of small- to moderate-magnitude volcanic
38 eruptions, anthropogenic sulphur emissions and transport processes over the period 1998-2012 and their role in
39 the warming hiatus. Two further experiments will investigate the stratospheric sulphate aerosol evolution after
40 major volcanic eruptions. The “Historical Eruptions SO₂ Emission Assessment” (HErSEA) experiment will



41 focus on the uncertainty in the initial emission of recent large-magnitude volcanic eruptions, while the
42 “Pinatubo Emulation in Multiple models” (PoEMS) experiment will provide a comprehensive uncertainty
43 analysis of the radiative forcing from the 1991 Mt. Pinatubo eruption.

44 **1 Introduction**

45 Stratospheric aerosol is an important component of the Earth system, which influences atmospheric radiative
46 transfer, composition and dynamics, thereby modulating the climate. The effects of stratospheric aerosol on
47 climate are especially evident when the opacity of the stratospheric aerosol layer is significantly increased after
48 volcanic eruptions. Through changes in the radiative properties of the stratospheric aerosol layer, volcanic
49 eruptions are a significant driver of climate variability (e.g. Myhre et al., 2013; Zanchettin et al., 2016). Major
50 volcanic eruptions inject vast amounts of SO₂ into the stratosphere, which is converted into sulphuric acid
51 aerosol with an e-folding time of about a month. Observations show that the stratospheric aerosol layer remains
52 enhanced for several years after major eruptions (SPARC, 2006). Such long-lasting volcanic perturbations cool
53 the Earth’s surface by scattering incoming solar radiation and warm the stratosphere by absorption of infrared
54 solar and long-wave terrestrial radiation which affect the dynamical structure as well as the chemical
55 composition of the atmosphere (e.g. Robock, 2000; Timmreck, 2012). As the ocean has a much longer memory
56 than the atmosphere, large volcanic eruptions could have a long lasting impact on the climate system that
57 extends beyond the duration of the volcanic forcing (e.g., Zanchettin et al., 2012; Swingedouw et al., 2017). The
58 chemical and radiative effects of the stratospheric aerosol are strongly influenced by its particle size distribution.
59 Heterogeneous chemical reactions, which most notably lead to substantial ozone depletion (e.g. WMO Ozone
60 Assessment 2007, chapter 3), take place on the surface of the stratospheric aerosol particles and are dependent
61 on the aerosol surface area density. Aerosol particle size determines the scattering efficiency of the particles
62 (e.g. Lacis et al., 1992).and their atmospheric lifetime (e.g., Pinto et al., 1989; Timmreck et al., 2010). Smaller-
63 magnitude eruptions than 1991 Mt. Pinatubo eruption can also have significant impacts on climate. It is now
64 established that a series of relatively small magnitude volcanic eruptions caused the increase in stratospheric
65 aerosol observed between 2000 and 2010 over that period based on ground- and satellite-borne observations
66 (Vernier et al., 2011b; Neely et al., 2013). Studies have suggested that this increase in stratospheric aerosol
67 partly counteracted the warming due to increased greenhouse gases over that period (e.g. Solomon et al., 2011;
68 Ridley et al., 2014; Santer et al., 2015).

69 Since the 2006 SPARC Assessment of Stratospheric Aerosol Properties Report (SPARC 2006, herein referred as
70 ASAP2006) the increase in observations of stratospheric aerosol and its precursor gases and in the number of
71 models which treat stratospheric aerosol interactively, have advanced scientific understanding of the
72 stratospheric aerosol layer and its effects on the climate (Kremser et al. 2016, herein referred to as KTH2016).
73 In particular, research findings have given to the community a greater awareness of the role of the tropical
74 tropopause layer (TTL) as a distinct pathway for transport into the stratosphere, of the interactions between
75 stratospheric composition and dynamics, and of the importance of moderate-magnitude eruptions in influencing



76 the stratospheric aerosol loading. In addition, over the last decade several new satellite instruments producing
77 observations relevant to the stratospheric aerosol layer have become operational. For example, we now have a
78 2002-2012 long record of global altitude-resolved SO₂ and OCS measurements provided by the Michelson
79 Interferometer for Passive Atmospheric Sounding Environmental Satellite (MIPAS Envisat, Höpfner et al.,
80 2013; 2015; Glatthor et al., 2015). Furthermore aerosol extinction vertical profiles are available from limb-
81 profiling instruments such as Scanning Imaging Absorption Spectrometer for Atmospheric Chartography
82 (SCIAMACHY, 2002-2012; Bovensmann et al., 1999; von Savigny et al., 2015), Optical Spectrograph and
83 InfraRed Imager System (OSIRIS, 2001-present, Bourassa et al., 2007), and Ozone Mapping and Profiler Suite-
84 Limb Profiler (OMPS-LP, 2011-present, Rault and Loughman, 2013), and from the active sensor lidar
85 measurements such as Cloud-Aerosol Transport System (CATS, 2015-present, Yorks et al., 2015) and Cloud-
86 Aerosol Lidar with Orthogonal Polarization (CALIOP, 2006-present, Vernier et al., 2009). Existing
87 measurements have become more robust, for example by homogenising the observations of aerosol properties
88 derived from optical particle counter (OPC) and satellite measurements during stratospheric aerosol background
89 periods (Kovilakam and Deshler, 2015), which previously showed large differences (Thomason et al., 2008).
90 Other efforts include combining and comparing different satellite data sets (e.g. Rieger et al., 2015). However,
91 some notable discrepancies still exist between different measurement datasets. For example, Reeves et al. (2008)
92 showed that aircraft-borne Focused Cavity Aerosol Spectrometer (FCAS) measurements of the particle size
93 distribution during the late 1990s yield surface area densities a factor 1.5 to 3 higher than that derived from
94 Stratospheric Aerosol and Gases Experiment (SAGE-II) measurements.

95 On the modelling side there has been an increasing amount of global three-dimensional stratospheric aerosol
96 models developed within the last years and used by research teams around the world (KTH2016). The majority
97 of these global models explicitly simulate aerosol microphysical processes and treat the full life cycle of
98 stratospheric aerosol, from the initial injection of sulphur containing gases, and their transformation into aerosol
99 particles, to their final removal from the stratosphere. Several of these models also include the interactive
100 coupling between aerosol microphysics, atmospheric chemistry, dynamics and radiation.

101 Given the improvements in observations and modelling of stratospheric aerosol since ASAP2006, we anticipate
102 further advances in our understanding of stratospheric aerosol by combining the recent observational record
103 with results from the current community of interactive stratospheric aerosol models. An Interactive
104 Stratospheric Aerosol Model Intercomparison Project (ISA-MIP) has therefore been developed within the
105 SSiRC framework. The SPARC activity Stratospheric Sulfur and its Role in Climate (SSiRC) (www.sparc-ssirc.org)
106 was initiated with the goal of reducing uncertainties in the properties of stratospheric aerosol and
107 assessing its climate forcing. In particular, constraining simulations of historical eruptions with available
108 observational datasets gives the potential to evaluate and substantially improve the accuracy of the volcanic
109 forcing datasets used in climate models. This will not only enhance consistency with observed stratospheric
110 aerosol properties and the underlying microphysical, chemical, and dynamical processes but also improve the
111 conceptual understanding. The use of such new volcanic forcing datasets has the potential to increase the



112 reliability of the simulated climate impacts of volcanic eruptions, which have been identified as a major
113 influence on decadal global mean surface temperature trends in climate models (Marotzke and Forster, 2015).
114 The first international model inter-comparison of global stratospheric aerosol models was carried out within
115 ASAP2006 and indicated that model simulations and satellite observations of stratospheric background aerosol
116 extinction agree reasonably well in the visible wavelengths but not in the infrared. It also highlighted systematic
117 differences between modelled and retrieved aerosol size, which are not able to detect the Aitken-mode sized
118 particles ($R < 50\text{nm}$) in the lower stratosphere (Thomason et al., 2008; Reeves et al., 2008; Hommel et al. 2011).
119 While in ASAP2006, only five global two- and three-dimensional stratospheric aerosol models were included in
120 the analysis, there are nowadays more than 15 global three-dimensional models worldwide available
121 (KTH2016). No large comprehensive model intercomparison has ever been carried out to identify differences in
122 stratospheric aerosol properties amongst these new interactive models. The models often show significant
123 differences in terms of their simulated transport, chemistry, and removal of aerosols with inter-model
124 differences in stratospheric circulation, radiative-dynamical interactions and exchange with the troposphere
125 likely to play an important role (e.g. Aquila et al., 2012; Niemeier and Timmreck, 2015). The formulation of
126 microphysical processes are also important (e.g. English et al. 2013), as are differing assumptions regarding the
127 sources of stratospheric aerosols and their precursors. A combination of these effects likely explain the large
128 inter-model differences as seen in Fig. 1 among global stratospheric aerosol models who participated in the
129 Tambora intercomparison, a precursor to the “consensus volcanic forcings” aspects of the CMIP6 Model
130 Intercomparison Project on the climatic response to Volcanic forcing (VolMIP, Zanchettin et al., 2016; Marshall
131 et al., 2017). Even for the relatively recent 1991 Mt. Pinatubo eruption, to reach the best agreement with
132 observations, interactive stratospheric models have used a wide range of SO_2 injections amounts, from as low at
133 10 Tg of SO_2 (Dhomse et al., 2014; Mills et al., 2016) to as high as 20 Tg of SO_2 (e.g. Aquila et al., 2012;
134 English et al., 2013).

135 Volcanic eruptions are commonly taken as a real-world analogue for hypothesised geoengineering via
136 stratospheric sulphur solar radiation management (SS-SRM). Indeed many of the assumptions and uncertainties
137 related to simulated volcanic perturbations to the stratospheric aerosol are also frequently given as caveats
138 around research findings from modelling studies which seek to quantify the likely effects from SS-SRM (e.g.
139 National Research Council, 2015), the mechanism-steps between sulphur injection and radiative cooling being
140 common to both aspects (Robock et al., 2013). The analysis of the ISA-MIP experiments we expect to improve
141 understanding of model sensitivities to key sources of uncertainty, to inform interpretation of coupled climate
142 model simulations and the next Intergovernmental Panel on Climate Change (IPCC) assessment. It will also
143 provide a foundation for co-operation to assess the atmospheric and climate changes when the next large-
144 magnitude eruption takes place.

145 In this paper, we introduce the new model intercomparison project ISA-MIP developed within the SSiRC
146 framework. In section 2 we provide an overview of the current state of stratospheric sulphur aerosol modelling
147 and its greatest challenges. In section 3 we describe the scopes and protocols of the four model experiments
148 planned within ISA-MIP. A concluding summary is provided in Section 4.



149 2. Modelling stratospheric aerosol; overview and challenges

150 Before we discuss the current state of stratospheric aerosol modelling and its greatest challenges in detail, we
151 briefly describe the main features of the stratospheric sulphur cycle. We are aware of the fact that the
152 stratospheric aerosol layer also contains organics and inclusions of meteoritic dust (Ebert et al., 2016) and, after
153 volcanic events, also co-exists with volcanic ash (e.g. Pueschel et al., 1994; KTH2016). However, the focus of
154 the ISA-MIP experiments described here is on comparing to measurements of the overall optical and physical
155 properties of the stratospheric aerosol layer, which is mainly determined by stratospheric aerosol.

156 2.1 The stratospheric aerosol lifecycle

157 The stratospheric aerosol layer and its temporal and spatial variability are determined by the transport of aerosol
158 and aerosol precursors in the stratosphere and their modification by chemical and microphysical processes
159 (Hamill et al., 1997; ASAP2006; KTH2016). Volcanic eruptions can inject sulphur-bearing gases directly into
160 the stratosphere which significantly enhances the stratospheric aerosol load for years. A number of observations
161 show that stratospheric aerosol increased over the first decade of the 21st century (e.g. Hofmann et al., 2009;
162 Vernier et al., 2011b; Ridley et al., 2014). Although such increase was attributed to the possible cause of Asian
163 anthropogenic emission increase (Hofmann et al., 2009), later studies have shown that small-to-moderate
164 magnitude volcanic eruptions are likely to be the major source of this recent increase (Vernier et al., 2011b;
165 Neely et al., 2013; Brühl et al., 2015).

166 A stratospheric source besides major volcanic eruptions is the photochemical oxidation of carbonyl sulphide
167 (OCS), an insoluble gas mainly inert in the troposphere. Tropospheric aerosols and aerosol precursor also enter
168 the stratosphere through the tropical tropopause and through convective updrafts in the Asian and North
169 American Monsoons (Hofmann et al., 2009; Hommel et al., 2011; Vernier et al., 2011a; Bourassa et al., 2012;
170 Yu et al., 2015). In the stratosphere, new sulphate aerosol particles are formed by binary homogenous nucleation
171 (Vehkamäki et al., 2002), a process in which sulphuric acid vapour ($\text{H}_2\text{SO}_4(\text{g})$) and water vapour condense
172 simultaneously to form a liquid droplet. The condensation of $\text{H}_2\text{SO}_4(\text{g})$ onto pre-existing aerosol particles and
173 the coagulation among particles shift the aerosol size distribution to greater radii. This takes place especially
174 under volcanically perturbed conditions, when the concentrations of aerosol in the stratosphere are higher (e.g.
175 Deshler et al., 2008).

176 From the tropics, where most of the tropospheric aerosol enters the stratosphere and the OCS chemistry is most
177 active, the stratospheric aerosol particles are transported poleward within the large-scale Brewer-Dobson
178 circulation (BDC) and removed through gravitational sedimentation and cross-tropopause transport in the extra-
179 tropical regions. Internal variability associated with the quasi-biennial oscillation (QBO) alters the isolation of
180 the tropical stratosphere and subsequently the extra-tropical transport of the stratospheric aerosol, and modifies
181 its distribution, particle size, and lifetime (e.g. Trepte and Hitchmann, 1992; Hommel et al., 2015).

182 In general, under volcanically perturbed conditions with larger amounts of injected SO_2 , aerosol particles grow
183 to much larger radii than in volcanic quiescent conditions (e.g. Deshler, 2008). Simulation of extremely large



184 volcanic sulphur rich eruptions show a shift to particle sizes even larger than observed after the Pinatubo
185 eruption, and predict a reduced cooling efficiency compared to moderate with moderate sulphur injections (e.g.
186 Timmreck et al., 2010; English et al., 2013).

187 **2.2 Global stratospheric aerosol models, current status and challenges**

188 A comprehensive simulation of the spatio-temporal evolution of the particle size distribution is a continuing
189 challenge for stratospheric aerosol models. Due to computational constraints, the formation of the stratospheric
190 aerosol and the temporal evolution of its size distribution are usually parameterized with various degrees of
191 complexity in global models. The simplest way to simulate the stratospheric aerosol distribution in global
192 climate models is the mass only (bulk) approach (e.g. Timmreck et al., 1999a; 2003; Aquila et al., 2012), where
193 only the total sulphate mass is prognostically simulated and chemical and radiative processes are calculated
194 assuming a fixed typical particle size distribution. More complex methods are size-segregated approaches, such
195 as the modal approach (e.g. Niemeier et al., 2009; Toohey et al., 2011; Brühl et al., 2012; Dhomse et al., 2014;
196 Mills et al., 2016), where the aerosol size distribution is simulated using one or more modes, usually of log-
197 normal shape. The mean radius of each mode of these size distributions varies in time and space. Another
198 common approach is the sectional method (e.g. English et al., 2011; Hommel et al., 2011; Sheng et al., 2015a;
199 for ref prior to 2006 see ASAP2006, chapter 5), where the particle size distribution is divided into distinct size
200 sections. Number and width of the size sections are dependent on the specific model configuration, but are fixed
201 throughout time and space. Size sections may be defined by an average radius, or by an average mass of
202 sulphur, and are often spaced geometrically.

203 The choice of methods has an influence on simulated stratospheric aerosol size distributions and therefore on
204 radiative and chemical effects. While previous model intercomparison studies in a box model (Kokkola et al.,
205 2009) or in a two-dimensional framework (Weisenstein et al., 2007) were very useful for the microphysical
206 schemes, they could not address uncertainties in the spatial transport pattern e.g. transport across the tropopause
207 and the subtropical transport barrier, or regional/local differences in wet and dry removal. These uncertainties
208 can only be addressed in a global three-dimensional model framework and with a careful validation with a
209 variety of observational data.

210 The June 1991 eruption of Mt. Pinatubo, with the vast net of observations that tracked the evolution of the
211 volcanic aerosol, provides a unique opportunity to test and validate global stratospheric aerosol models and their
212 ability to simulate stratospheric transport processes. Previous model studies (e.g. Timmreck et al., 1999b; Aquila
213 et al., 2012) highlighted the importance of an interactive online treatment of stratospheric aerosol radiative
214 heating for the simulated transport of the volcanic cloud. A crucial point is the simulation of the tropical
215 stratospheric aerosol reservoir (i.e., the tropical pipe, Plumb, 1996) and the meridional transport through the
216 subtropical transport barrier. Some models show a very narrow tropical maximum in comparison to satellite data
217 (e.g., Dhomse et al. 2014) while others show too fast transport to higher latitudes and fail to reproduce the long
218 persistence of the tropical aerosol reservoir (e.g. Niemeier et al., 2009; English et al., 2013). Reasons for these
219 differences need to be understood.



220 3. The ISA-MIP Experiments

221 Many uncertainties remain in the model representation of stratospheric aerosol. Figure 2 summarizes the main
222 processes that determine the stratospheric sulphate aerosol mass load, size distribution and the associated optical
223 properties. The four experiments in ISA-MIP are designed to address these key processes under a well-defined
224 experiment protocol with prescribed boundary conditions (sea surface temperatures (SSTs), emissions). All
225 simulations will be compared to observations to evaluate model performances and understand model strengths
226 and weaknesses. The experiment “Background” (BG) focuses on microphysics and transport (section 3.1) under
227 volcanically quiescent conditions, when stratospheric aerosol is only modulated by seasonal changes and
228 interannual variability. The experiment “Transient Aerosol Record” (TAR) is addressing the role of time-
229 varying SO₂ emission in particular the role of small- to moderate-magnitude volcanic eruptions and transport
230 processes in the upper troposphere – lower stratosphere (UTLS) over the period 1998-2012 (section 3.2). Two
231 further experiments investigate the stratospheric sulphate aerosol size distribution under the influence of large
232 volcanic eruptions. “HERSEA” focuses on the uncertainty in the initial emission characteristics of recent large
233 volcanic eruptions (section 3.3), while “PoEMS” provides an extensive uncertainty analysis of the radiative
234 forcing of the Mt. Pinatubo eruption. In particular the ISA-MIP model experiments aim to address the following
235 questions:

- 236 1. How large is the stratospheric sulphate load under volcanically quiescent conditions, and how sensitive
237 is the simulation of this background aerosol layer to model specific microphysical parameterization and
238 transport? (3.1)
- 239 2. Can we explain the sources and mechanisms behind the observed variability in stratospheric aerosol
240 load since the year 2000? (3.2)
- 241 3. Can stratospheric aerosol observations constrain uncertainties in the initial sulphur injection amount
242 and altitude distribution of the three largest volcanic eruptions of the last 100 years? (3.3)
- 243 4. What is the confidence interval for volcanic forcing of the Pinatubo eruption simulated by interactive
244 stratospheric aerosol models and to which parameter uncertainties are the predictions most sensitive to?
245 (3.4)

246 Table 1 gives an overview over all ISA-MIP experiments, which are described in detail below. In general each
247 experiment will include several simulations from which only a subset is mandatory (Tier1). The modelling
248 groups are free to choose in which of the experiments they would like to participate, however the BG Tier1
249 simulation is mandatory for all groups and the entry card for the ISA-MIP intercomparison. All model results
250 will be saved in a consistent format (NETCDF) and made available via <http://cera-www.dkrz.de/WDCC/ui>, and
251 compared to a set of benchmark observations. More detail technical information about data requests can be
252 found in the supplementary material and on the ISA-MIP webpage: <http://www.isamip.eu>.

253 It is mandatory for participating models to run with interactive sulphur chemistry (see review in SPARC
254 ASAP2006) in order to capture the oxidation pathway from precursors to aerosol particles, including aerosol



255 growth due to condensation of H_2SO_4 . Chemistry Climate Models (CCMs) with full interactive chemistry follow
256 the Chemistry Climate Initiative (CCMI) hindcast scenario REF-C1 (Eyring et al. 2013,
257 http://www.met.reading.ac.uk/ccmi/?page_id=11) for the treatment of chemical fields and emissions of
258 greenhouse gases (GHGs), ozone depleting substances (ODSs), and very short-lived substances (VSLs). Sea
259 surface temperatures and sea ice extent are prescribed as monthly climatologies from the MetOffice Hadley
260 Center Observational Dataset (Rayner et al. 2003). An overview of the boundary conditions is included in the
261 supplementary material (Table S1). Table S2 reports the inventories to be used for tropospheric emissions of
262 aerosols and aerosol precursors. Anthropogenic sulphur emissions and biomass burning are taken from the
263 Monitoring Atmospheric Composition and Climate (MACC)-CITY climatology (Granier et al., 2011). S
264 emissions from continuously erupting volcanoes are taken into account using Dentener et al. (2006) which is
265 based on Andres and Kasgnoc (1998). OCS concentrations are fixed at the surface at a value of 510 pptv
266 (Montzka et al., 2007; ASAP2006). If possible, DMS, dust, and sea salt emissions should be calculated online
267 depending on the model meteorology. Models considering DMS oxidation should calculate seawater DMS
268 emissions as a function of wind speed and DMS seawater concentrations. Otherwise, modelling groups should
269 prescribe for these species their usual emission database for the year 2000. Each group can specify solar forcing
270 for year 2000 conditions according to their usual dataset.
271 Modelling groups are encouraged to include a set of passive tracers to diagnose the atmospheric transport
272 independently from emissions mostly following the CCMI recommendations (Eyring et al., 2013). These tracers
273 are listed in Table S3 in the supplementary material. Models diagnose aerosol parameters as specified in Tables
274 S4, S5. Additionally, volume mixing ratios of specified precursors are diagnosed

275 **3.1 Stratospheric Background Aerosol (BG)**

276 **3.1.1. Summary of experiment**

277 The overall objective of the BG experiment is to better understand the processes involved in maintaining the
278 stratospheric background aerosol layer, i.e. stratospheric aerosol not resulting from direct volcanic injections
279 into the stratosphere. The simulations prescribed for this experiment are time-slice simulations for the year 2000
280 with prescribed SST including all sources of aerosols and aerosol-precursors except for explosive volcanic
281 eruptions. The result of BG will be a multi-model climatology of aerosol distribution, composition, and
282 microphysical properties in absence of volcanic eruptions. By comparing models with different aerosol
283 microphysics parameterization and simulations of background circulation with a variety of observational data
284 (Table 2), we aim to assess how these processes impact the simulated aerosol characteristics.

285 **3.1.2. Motivation**

286 The total net sulphur mass flux from the troposphere into the stratosphere is estimated to be about 181 Gg S/yr
287 based on simulations by Sheng et al. (2015a) using the SOCOL-AER model, 1.5 times larger than reported in
288 ASAP2006 (KTH2016). This estimate, however, could be highly dependent on the specific characteristics of the



289 model used, such as strength of convective systems, scavenging efficiency, and occurrence of stratosphere-
290 troposphere exchange. Therefore, the simulated distribution of stratospheric background aerosol could show,
291 especially in the lower stratosphere, a very large inter-model variability.

292 OCS is still considered the largest contributor to the aerosol loadings in the middle stratosphere. Several studies
293 have shown that the transport to the stratosphere of tropospheric aerosol and aerosol precursors constitutes an
294 important source of stratospheric aerosol (KTH2016 and references herein) although new in situ measurements
295 indicate the SO₂ flux cross the tropopause is negligible over Mexico and central America (Rollins et al., 2017).
296 Observations of the Asian Tropopause Aerosol Layer (ATAL, Vernier et al., 2011a) show that, particularly in
297 the UTLS, aerosol of tropospheric origin can significantly enhance the burden of aerosol in the stratosphere.
298 This tropospheric aerosol has a more complex composition than traditionally assumed for stratospheric aerosol:
299 Yu et al. (2015), for instance, showed that carbonaceous aerosol makes up to 50% of the aerosol loadings within
300 the ATAL. The rate of stratospheric-tropospheric exchange (STE) is influenced by the seasonality of the
301 circulation and the frequency and strength of convective events in large-scale phenomena such as the Asian and
302 North American monsoon or in small-scale phenomena such as strong storms. Model simulations by Hommel et
303 al. (2015) also revealed significant QBO signatures in aerosol mixing ratio and size in the tropical middle
304 stratosphere (Figure 3). Hence, the model specific implementation of the QBO (nudged or internally generated)
305 could impact its effects on the stratospheric transport and, subsequently, on the stratospheric aerosol layer.

306 In this experiment, we aim to assess the inter-model variability of the background stratospheric aerosol layer,
307 and of the sulphur mass flux from the troposphere to the stratosphere and vice versa. We will exclude changes in
308 emissions and focus on the dependence of stratospheric aerosol concentrations and properties on stratospheric
309 transport and stratosphere-troposphere exchange (STE). The goal of the BG experiment aims to understand how
310 the model-specific transport characteristics (e.g. isolation of the tropical pipe, representation of the QBO and
311 strength of convective systems) and aerosol parameterizations (e.g. aerosol microphysics and scavenging
312 efficiency) affect the representation of the background aerosol.

313 3.1.3. Experiment setup and specifications

314 The BG experiment prescribes one mandatory (BG_QBO) and two recommended (BG_NQBO and BG_NAT)
315 simulations (see Table 3). BG_QBO is a time slice simulation with conditions characteristic of the year 2000¹,
316 with the goal of understanding sources, sinks, composition, and microphysical characteristics of stratospheric
317 background aerosol under volcanically quiescent conditions. The time-slice simulation should be at least 20 year
318 long, after a spin-up period of at least 10 years to equilibrate stratospheric relevant quantities such as OCS
319 concentrations and age of air. The period seems to be sufficient to study differences in the aerosol properties but
320 need to extended if dynamical changes e.g. in NH winter variability will be analysed. Modelling groups should
321 run this simulation with varying QBO, either internally generated or nudged to the 1980-2000 period.

¹ To ensure comparability to the AeroCom simulations (<http://aerocom.met.no/Welcome.html>)



322 If resources allow, each model should perform the sensitivity experiments BG_NQBO and BG_NAT. The
323 specifics of these two experiments are the same as for BG_QBO, but BG_NQBO should be performed without
324 varying QBO² and BG_NAT without anthropogenic emissions of aerosol and aerosol precursors, as indicated in
325 Table S1. The goals of these sensitivity experiments are to understand the effect of the QBO on the background
326 aerosol characteristics and the contribution of anthropogenic sources to the background aerosol loading in the
327 stratosphere.

328 **3.2 Transient Aerosol Record (TAR)**

329 **3.2.1 Summary of experiment**

330 The aim of the TAR (Transient Aerosol Record) experiment is to investigate the relative contributions of
331 volcanic and anthropogenic sources to the temporal evolution of the stratospheric aerosol layer between 1998
332 and 2012. Observations show that there is a transient increase in stratospheric aerosol loading, in particular after
333 the year 2003, with small-to moderate-magnitude volcanic eruptions contributing significantly to this increase
334 (e.g. Solomon et al., 2011; Vernier et al., 2011b; Neely et al., 2013; Ridley et al. 2014; Santer et al., 2015; Brühl
335 et al., 2015). TAR model simulations will be performed using specified dynamics, prescribed sea surface
336 temperature and time-varying SO₂ emissions. The simulations are suitable for any general circulation or
337 chemistry transport models that simulate the stratospheric aerosol interactively and have the capability to nudge
338 meteorological parameters to reanalysis data. The TAR protocol covers the period from January 1998 to
339 December 2012, when only volcanic eruptions have affected the upper troposphere and lower stratosphere
340 (UTLS) aerosol layer with SO₂ emissions about an order of magnitude smaller than Pinatubo. Time-varying
341 surface emission datasets contain anthropogenic and natural sources of sulphur aerosol and their precursor
342 species. The volcanic SO₂ emission inventories contain information of all known eruptions that emitted SO₂ into
343 the UTLS during this period. It comprises the geolocation of each eruption, the amount of SO₂ emitted, and the
344 height of the emissions. SO₂ emissions from continuously-degassing volcanoes are also included.

345 **3.2.2 Experiment setup and specifications**

346 Participating models are encouraged to perform up to seven experiments, based on five different volcanic SO₂
347 emission databases (hereafter referred to as VolcDB). Four experiments are mandatory, three other are optional.
348 The volcanic experiments are compared to a reference simulation (noVolc) that does not use any of the volcanic
349 emission databases, but emissions from continuously-degassing volcanoes. The aim of the reference simulation
350 is to simulate the non-volcanically perturbed state of the stratospheric aerosol layer. In contrast to the
351 experiment protocol BG (Section 3.1), here time-varying surface boundary conditions (SST/SIC) are applied,
352 whereas BG intercompares model simulations under climatological mean conditions and uses constant 2000
353 conditions.

² Models with an internal generated QBO might nudge the tropical stratospheric winds.



354 An overview of the volcanic emission inventories is given in Table 4 and in Figure 4 VolcDB1/2/3 are new
355 compilations (Bingen et al., 2017; Neely and Schmidt, 2016; Carn et al., 2016), whereas a fourth inventory
356 (VolcDB4; Diehl et al., 2012), provided earlier, for the AeroCom community modelling initiative, is optional.
357 The databases use SO₂ observations from different sources and apply different techniques for the estimation of
358 injection heights and the amount of emitted SO₂. The 4 inventories are provided in the form of tabulated point
359 sources, with each modelling group t

360 o translate emitted SO₂ mass for each eruption into model levels spanning the upper and lower emission
361 altitudes. If modelling groups prefer not to use point sources, we additionally offer VolcDB1_3D which
362 provides a series of discrete 3D gridded SO₂ injections at specified times. In both versions of VolcDB1, the
363 integral SO₂ mass of each injection is consistent.

364 We recommend performing one additional non-mandatory experiment in order to quantify and isolate the effects
365 of 8 volcanic eruptions that either had a statistically significant effect on, for instance, tropospheric temperatures
366 (Santer et al., 2014, 2015) or emitted significant amounts of SO₂ over the 1998 to 2012 time period. This
367 experiment uses a subset of volcanic emissions (VolcDBSUB), that were derived based on the average mass of
368 SO₂ emitted using VolcDB1, VolcDB2, and VolcDB3 for the following eruptions: 28 January 2005 Manam
369 (4.0S, Papua New Guinea), 7 October 2006 Tavurvur (4.1 S, Papua New Guinea), 21 June 2009 Sarychev,
370 (48.5° N, Kyrill, UDSSR) 8 November 2010 Merapi (7.3° S, Java, Indonesia), and 21 June 2011 Nabro (13.2°
371 N, Eritrea). In addition the eruptions of Soufriere Hills (16.4° N, Monserrat) on 20 May 2006, Okmok (53.3° N,
372 Alaska) on 12 July 2008 and Kasatochi (52.1° N, Alaska) on 7 August 2008 are considered although these are
373 not discernible in climate proxy (Kravitz and Robock, 2010; Santer et al., 2014; 2015).

374 Summarising the number of experiments to be conducted within TAR: four are mandatory (noVolc,
375 VolcDB1/2/3), one additional is recommended (VolcDBSUB) and two others are optional (VolcDB4 and
376 VolcDB1_3D; see Table 5 for an overview).

377 ***Volcanic SO₂ Emission Databases***

378 VolcDB1 (Bingen et al., 2017 and Table S6) are updates from Brühl et al. (2015) using satellite data of MIPAS
379 and OMI. For TAR, VolcDB1 has been extended based on data from Global Ozone Monitoring by Occultation
380 of Stars (GOMOS), SAGE II, Total Ozone Mapping Spectrometer (TOMS), and the Smithsonian database. The
381 optionally provided VolcDB1_3D data set, contains volume mixing ratio distributions of the injected SO₂ on a
382 T42 Gaussian grid with 90 levels. VolcDB2 (Mills et al., 2016; Neely and Schmidt, 2016) contains volcanic SO₂
383 emissions and plume altitudes for eruptions between that have been detected by satellite instruments including
384 TOMS, OMI, OMPS, Infrared Atmospheric Sounding Interferometer (IASI), Global Ozone Monitoring
385 Experiment (GOME/2), Atmospheric Infrared Sounder (AIRS), Microwave Limb Sounder (MLS) and the
386 MIPAS instrument. The database is compiled based on published estimates of the eruption source parameters
387 and reports from the Smithsonian Global Volcanism Program (<http://volcano.si.edu/>), NASA's Global Sulfur
388 Dioxide Monitoring website (<http://so2.gsfc.nasa.gov/>) as well as the Support to Aviation Control Service
389 (<http://sacs.aeronomie.be/>). The tabulated point source database also includes volcanic eruptions that emitted



390 SO₂ into the troposphere only, as well as direct stratospheric emissions and has been used and compared to
391 observations in Mills et al. (2016) and Solomon et al. (2016).
392 VolcDB3 uses the most recent compilation of the volcanic degassing data base of Carn et al. (2016).
393 Observations from the satellite instruments TOMS, the High-resolution Infrared Sounder (HIRS/2), AIRS, OMI,
394 MLS, IASI and OMPS are considered, measuring in the UV, IR and microwave spectral bands. Similar to
395 VolcDB1/2, VolcDB3 also includes tropospheric eruptions.
396 Historically VolcDB4 is an older dataset, which relies on information from OMI, the Global Volcanism
397 Program (GVP), and other observations from literature, covering time period from 1979 to 2010. In contrast to
398 the other inventories, VolcDB4 has previously been applied by a range of models within the AeroCom,
399 community (<http://aerocom.met.no/emissions.html>; Diehl et al., 2012, Dentener et al., 2006). Hence, it adds
400 valuable information to the TAR experiments because it allows estimating how the advances in observational
401 methods impact modelling results. It should be noted that VolcDB4 already contains the inventory of Andres
402 and Kasgnoc (1998) for S emissions from continuously erupting volcanoes and should not be allocated twice
403 when running this experiment.

404 *Boundary Conditions, Chemistry and Forcings*

405 To reduce uncertainties associated with model differences in the reproduction of synoptic and large-scale
406 transport processes, models are strongly encouraged to perform TAR experiments with specified dynamics,
407 where meteorological parameters are nudged to a reanalysis such as the ECMWF ERA-Interim (Dee et al.,
408 2011). This allows models to reasonably reproduce the QBO and planetary wave structure in the stratosphere
409 and to replicate as closely as possible the state of the BDC in the simulation period. Nudging also allows
410 comparing directly to available observations of stratospheric aerosol properties (Table 2), such as the extinction
411 profiles and AOD, and should enable the models to simulate the Asian tropopause layer (ATAL; Vernier et al.,
412 2011a; Thomason and Vernier, 2013), which, so far, has been studied only by very few global models in great
413 detail (e.g. Neely et al., 2014; Yu et al., 2015).

414

415 **3.3. Historical Eruption SO₂ Emission Assessment" (HErSEA)**

416 **3.3.1 Summary of experiment**

417 This Historical Eruption SO₂ Emission Assessment (HErSEA) experiment will involve each participating model
418 running a limited ensemble of simulations for each of the three largest volcanic perturbations to the stratosphere
419 in the last 100 years: 1963 Mt. Agung, 1982 El Chichón and 1991 Mt. Pinatubo.

420 The main aim is to use a wide range of stratospheric aerosol observations to constrain uncertainties in the SO₂
421 emitted for each eruption (amount, injection height). Several different aerosol metrics will be intercompared to
422 assess how effectively the emitted SO₂ translates into perturbations to stratospheric aerosol properties and
423 simulated radiative forcings across interactive stratospheric aerosol CCMs with a range of different
424 complexities. Whereas the TAR simulations (see section 3.2) use specified dynamics, and are suitable for



425 chemistry transport models, for this experiment, simulations must be free-running with radiative coupling to
426 volcanically-enhanced stratospheric aerosol, thereby ensuring the composition-radiation-dynamics interactions
427 associated with the injection are resolved. We are aware that this specification inherently excludes chemistry
428 transport models, which must impose atmospheric dynamics. However, since the aim is to apply stratospheric
429 aerosol observations in concert with the models to re-evaluate current best-estimates of the SO₂ input, and in
430 light of the first order impact the stratospheric heating has on hemispheric dispersion from these major eruptions
431 (e.g. Young, R. E. et al., 1994), we assert that this apparent exclusivity is entirely justified in this case.

432 As well as analysing and evaluating the individual model skill and identifying model consensus and
433 disagreement for these three specific eruptions, we also seek to learn more about major eruptions which
434 occurred before the era of satellite and in-situ stratospheric measurements. Our understanding of the effects
435 from these earlier eruptions relies on deriving volcanic forcings from proxies such as sulphate deposition to ice
436 sheets (Gao et al., 2007; Sigl et al., 2015; Toohey et al., 2013), from photometric measurements from
437 astronomical observatories (Stothers, 1996, 2001) or from documentary evidence (Stothers, 2002; Stothers and
438 Rampino, 1983; Toohey et al., 2016a).

439 3.3.2 Motivation

440 In the days following the June 1991 Pinatubo eruption, satellite SO₂ measurements show (e.g. Guo et al.,
441 2004a) that the peak gas phase sulphur loading was 7 to 11.5 Tg [S] (or 14 -23 Tg SO₂). The chemical
442 conversion to sulphuric aerosol that occurred in the tropical reservoir over the following weeks, and the
443 subsequent transport to mid- and high-latitudes, caused a major enhancement to the stratospheric aerosol layer.
444 The peak particle sulphur loading, through this global dispersion phase, reached only around half that in the
445 initial SO₂ emission, the maximum particle sulphur loading measured as 3.7 to 6.7 Tg [S] (Lambert et al., 1993;
446 Baran and Foot, 1994), based on an aqueous sulphuric acid composition range of 59 to 77% by weight (Grainger
447 et al., 1993).

448 Whereas some model studies with aerosol microphysical processes find consistency with observations for SO₂
449 injection values of 8.5 Tg S (e.g., Niemeier et al., 2009; Toohey et al., 2011; Brühl et al., 2015), several recent
450 microphysical model studies (Dhomse et al., 2014; Sheng et al. 2015a; Mills et al., 2016) find best agreement
451 for an injected sulphur amount at, or even below, the lower end of the range from the satellite SO₂
452 measurements. Model predictions are known to be sensitive to differences in assumed injection height (e.g.
453 Sheng et al., 2015b, Jones et al., 2016) and whether models resolve radiative heating and “self-lofting” effects
454 also affects subsequent transport pathways (e.g. Young, R. E. et al., 1994; Timmreck et al. 1999b; Aquila et al.,
455 2012). Another potential mechanism that could explain part of the apparent model-observation discrepancy is
456 that a substantial proportion of the sulphur may have been removed from the plume in the first months after the
457 eruption due to accommodation onto co-emitted ash/ice (Guo et al., 2004b) and subsequent sedimentation.

458 This ISA-MIP experiment will explore these issues further, with the participating models carrying out co-
459 ordinated experiments of the three most recent major eruptions, with specified common SO₂ amounts and
460 injection heights (Table 6). This design ensures the analysis can focus on key inter-model differences such as



461 stratospheric circulation/dynamics, the impacts from radiative-dynamical interactions and the effects of aerosol
462 microphysical schemes. Analysing how the vertical profile of the enhanced stratospheric aerosol layer evolves
463 during global dispersion and decay, will provide a key indicator for why the models differ, and what are the key
464 driving mechanisms. For all three major eruptions, we have identified key observational datasets (Table 7) that
465 will provide benchmark tests to evaluate the vertical profile, covering a range of different aerosol metrics.

466 3.3.3 Experiment setup and specifications

467 Each modelling group will run a mini-ensemble of transient AMIP-type runs for the 3 eruptions with upper and
468 lower bound SO₂ emissions and 3 different injection height settings: two shallow (e.g. 19-21 km and 23-25 km)
469 and one deep (e.g. 19-25 km) (see Table 7). The seasonal cycle of the Brewer Dobson circulation affects the
470 hemispheric dispersion of the aerosol plume (e.g. Toohy et al., 2011) and the phase of the QBO is also known
471 to be key control for tropical eruptions (e.g. Trepte and Hitchman, 1992). To quantify the contribution of the
472 tracer transport, a passive tracer Volc (Table S3) will be additionally initialized. Note since the AMIP-type
473 simulations will be transient, prescribing time-varying sea-surface temperatures, the models will automatically
474 match the surface climate state (ENSO, NAO) through each post-eruption period. Where possible, models
475 should re-initialise (if they have internally generated QBO) or use specified dynamics approaches (e.g. Telford
476 et al., 2008) to ensure the model dynamics is consistent with the QBO evolution through the post-eruption
477 period. General circulation models should use GHG concentrations appropriate for the period and models with
478 interactive stratospheric chemistry should ensure the loading of Ozone Depleting Substances (ODSs) matches
479 that for the time period.

480 Table 8 shows the settings for the SO₂ injection for each eruption- Note that experience of running interactive
481 stratospheric aerosol simulations shows that the vertical extent of the enhanced stratospheric aerosol will be
482 different from the altitude range in which the SO₂ is injected. So, these sensitivity simulations will allow to
483 assess the behaviour of the individual models with identical settings for the SO₂ injection.

484 For these major eruptions, where the perturbation is much larger than in TAR, model diagnostics include AOD
485 and extinction at multiple wavelengths and heating rates (K/day) in the lower stratosphere to identify the
486 stratospheric warming induced by simulated volcanic enhancement, including exploring compensating effects
487 from other constituents (e.g. Kinne et al., 1992). To allow the global variation in size distribution to be
488 intercompared, models will also provide 3D-monthly effective radius, with also cumulative number
489 concentration at several size-cuts for direct comparison to balloon measurements. Examining the co-variation of
490 the particle size distribution with variations in extinction at different wavelengths will be of particular interest in
491 relation to approaches used to interpret astronomical measurements of eruptions in the pre-in-situ era (Stothers,
492 1996, 2001). A 3-member ensemble will be submitted for each different injection setting.

493

494 3.4. Pinatubo Emulation in Multiple models” (PoEMs)



495 **3.4.1 Summary of experiment**

496 The PoEMS experiment will involve each interactive stratospheric aerosol model running a perturbed parameter
497 ensemble (PPE) of simulations through the 1991-1995 Pinatubo-perturbed period. Variation-based sensitivity
498 analysis will derive a probability distribution function (PDF) for each model's predicted Pinatubo forcing,
499 following techniques applied successfully to quantify and attribute sources of uncertainty in tropospheric aerosol
500 forcings (e.g. Carslaw et al., 2013). The approach will teach us which aspects of the radiative forcing from
501 major eruptions is most uncertain, and will enable us to identify how sensitive model predictions of key features
502 (e.g. timing and value of peak forcing and decay timescales) are to uncertainties in several model parameters.
503 By comparing the time-signatures of different underlying aerosol metrics (mid-visible AOD, effective radius,
504 particle number) between models, and crucially also against observations, may also help to reduce the natural
505 forcing uncertainty, potentially thereby making the next generation of climate models more robust.

506 **3.4.2 Motivation**

507 The sudden global cooling from major eruptions is a key signature in the historical climate record and a natural
508 global warming signature occurs after peak cooling as volcanic aerosol is slowly removed from the stratosphere.
509 Quantitative information on the uncertainty range of volcanic forcings is therefore urgently needed. The amount
510 of data collected by satellite-, ground-, and air-borne instruments in the period following the 1991 eruption of
511 Mount Pinatubo (see e.g. section 3.3.2, Table 7) provides an opportunity to test model capabilities in simulating
512 large perturbations of stratospheric aerosol and their effect on the climate. Recent advances in quantify
513 uncertainty in climate models (e.g. Rougier et al., 2009; Lee et al. 2011) involve running ensembles of
514 simulations to systematically explore combinations of different external forcings to scope the range of possible
515 realisations. There are now a large number of general circulation models (GCMs) with prognostic aerosol
516 modules, which tend to assess the stratospheric aerosol perturbation through the Pinatubo-perturbed period (see
517 Table 9). Although these different models achieve reasonable agreement with the observations, this consistency
518 of skill is achieved with considerable diversity in the values assumed for the initial magnitude and distribution
519 of the SO₂ injection. The SO₂ injections prescribed by different models range from 5Tg-S to 10 Tg-S, and the
520 upper edge of the injection altitude varies among models from as low as 18km to as high as 29km, as shown in
521 Table 9. Such simulations also differ in the choice of the vertical distribution of SO₂ injection (e.g. uniform,
522 Gaussian, or triangular distributions) and the horizontal injection area (one to several grid boxes). The fact that
523 different choices of injection parameters lead to similar results in different models points to differences in the
524 models' internal treatment of aerosol evolution. Accurately capturing microphysical processes such as
525 coagulation, growth and subsequent rates of sedimentation has been shown to be important for volcanic
526 forcings (English et al., 2013), but some studies (e.g. Mann et al., 2015) identify that these processes interplay
527 also with aerosol-radiation interactions, the associated dynamical effects changing the fate of the volcanic
528 sulphur and its removal into the troposphere. The PoEMS experiment will specifically assess this issue by
529 adjusting the rate of specific microphysical processes in each model simultaneously with perturbations to SO₂



530 emission and injection height, thereby assessing the footprint of their influence on subsequent volcanic forcing
531 in different complexity aerosol schemes and the relative contribution to uncertainty from emissions and
532 microphysics.

533 3.4.3 Experiment setup and specifications

534 For each model, an ensemble of simulations will be performed varying SO₂ injection parameters and a selection
535 of internal model parameters within a realistic uncertainty distribution. A maximin Latin hypercube sampling
536 strategy will be used to define parameter values to be set in each PPE member in order to obtain good coverage
537 of the parameter space. The maximin Latin hypercube is designed such that the range of every single parameter
538 is well sampled and the sampling points are well spread through the multi-dimensional uncertainty space – this
539 is achieved by splitting the range of every parameter into N intervals and ensuring that precisely one point is in
540 each interval in all dimensions, where N is the total number of model simulations, and the minimum distance
541 between any pair of points in all dimensions is maximised. Fig. 6 shows the projection onto two dimensions of a
542 Latin hypercube built in 8 dimensions with 50 model simulations. The size of the Latin hypercube needed will
543 depend on the number of model parameters to be perturbed; the number of simulations to be performed will be
544 equal to seven times the number of parameters. All parameters are perturbed simultaneously in the Latin
545 hypercube.

546 In order to be inclusive of modelling groups with less computing time available, and different types of aerosol
547 schemes, we define 3 options of experimental design with different numbers of perturbed parameters and thus
548 simulation ensemble members. The 3 options involve varying all 8 (standard set), 5 (reduced set), or 3
549 (minimum set) of the list of uncertain parameters, resulting in ensembles of 64 (standard), 40 (reduced) or 24
550 (minimum) PPE members. The parameters to be varied are shown in Table 10, and include variables related to
551 the volcanic injection, such as its magnitude, height, latitudinal extent, and composition, and to the life cycle of
552 the volcanic sulphate, such as the sedimentation rate, its microphysical evolution, and the SO₂ to SO₄²⁻
553 conversion rate.

554 Prior to performing the full PPE, modelling groups are encouraged to run “One-At-a-Time” (OAT) test runs
555 with each of the process parameters increased/decreased to its maximum/minimum value. Submission of these
556 OAT test runs is encouraged (following the naming convention in Table 11) because as well as being an
557 important check that the model parameter-scaling is being implemented as intended, the results will also enable
558 intercomparison of single-parameter effects between participating models ahead of the full ensemble. That this
559 restriction to the parameter-scalings is operational is an important preparatory exercise and will need to have
560 been verified when running the OAT test runs.

561 Once a modelling group has performed the PPE of simulations as defined by the Latin hypercube a statistical
562 analysis will be performed. Emulators for each of a selection of key metrics will be built, following the
563 approach described by Lee et al. (2011), to examine how the parameters lead to uncertainty in key features of
564 the Pinatubo-perturbed stratospheric aerosol. The emulator builds a statistical model between the ensemble



565 design and the key model output and once validated allows sampling of the whole parameter space to derive a
566 PDF of each key model output.

567 Variance-based sensitivity analysis will then be used to decompose the resulting probability distribution into its
568 sources providing information on the key sources of uncertainty in any model output. The two sensitivity indices
569 of interest are called the main effect and the total effect. The main effect measures the percentage of uncertainty
570 in the simulated metric due to each parameter-variation individually. The total effect measures the percentage of
571 uncertainty in the key model output due to each parameter, including the additional contribution from its
572 interaction with other uncertain parameters. The sources of model parametric uncertainty (i.e. the sensitivity
573 indices) will be identified for each model with discussion with each group to check the results. By then
574 comparing the sensitivity to the uncertain parameters across the range of participating models, we will learn
575 about how the model's differing treatment of aerosol processes, and the inherent dynamical and chemical
576 processes resolved in the host model, together determine the uncertainty in its predicted Pinatubo radiative
577 forcings.

578 The probability distribution of observable key model outputs will also be compared to observations, in order to
579 constrain the key sources of uncertainty and thereby reduce the parametric uncertainty in individual models. The
580 resulting model constraints will be compared between models providing quantification of both parametric
581 uncertainty and structural uncertainty for key variables such as AOD, effective radius and radiative flux
582 anomalies. This sensitivity analysis will also identify the variables for which better observational constraints
583 would yield the greatest reduction in model uncertainties.

584

585 **4. Conclusions**

586 The ISA-MIP experiments will improve understanding of stratospheric aerosol processes, chemistry, and
587 dynamics, and constrain climate impacts of background aerosol “variability”, small volcanic eruptions, and
588 large volcanic eruptions. The experiments will also help to resolve some disagreements amongst global aerosol
589 models, for instance the difference in volcanic SO₂ forcing efficacy for Pinatubo (see section 3.3.2). The results
590 of this work will help constrain the contribution of stratospheric aerosols to the early 21st century global
591 warming hiatus period, the effects from hypothetical geoengineering schemes, and other climate processes that
592 are influenced by the stratosphere. Overall they provide an excellent opportunity to answer some of these
593 questions as part of the greater WCRP SPARC and CMIP6 efforts.

594 As well as identifying areas of agreement and disagreement among the different complexities of models in top-
595 level comparisons focussing on fields such as zonal-mean mid-visible AOD and extinction profiles in different
596 latitudes, we also intend to explore relationships between key parameters. For example, how does sulphate
597 deposition to the polar ice sheets relate to volcanic forcing in the different interactive stratospheric aerosol
598 models that predict the transport and sedimentation of the particles? Or how do model “spectral extinction
599 curves” evolve through the different volcanically-perturbed periods and how do they relate to simulated
600 effective radius compared to the theoretical approach to derive effective radius from Stothers (1997; 2001).

601 There is considerable potential to apply the model uncertainty analysis to make new statements to inform our



602 confidence of volcanic forcings derived from ice core and astronomical measurements for eruptions before the
603 in-situ measurement era.

604

605 **Code and data availability**

606 The model output from the all simulations described in this paper will be distributed through the World Data
607 climate Center <https://www.dkrz.de/up/systems/wdch> with digital object identifiers (DOIs) as-signed. The
608 model output will be freely accessible through this data portal after registration.

609

610 **Authorcontributions.**

611 CT, GWM VA, RH, LAL, AS, CB, SC MC, SSD, TD, JME, MJM, RN, JXS, MT and D.W designed the
612 experiments. CT and GWM coordinated the writing, and drafted the manuscript. All authors have contributed to
613 the writing and have approved of the final version of the manuscript.

614

615 **Competing interests.**

616 The authors declare that they have no conflict of interest.

617 **Acknowledgements**

618 The authors thank their SSiRC colleagues for continuing support and discussion. We acknowledge the scientific
619 guidance (and sponsorship) of the World Climate Research Programme to motivate this work, to be coordinated
620 in the framework of SPARC. C. Timmreck, M. Toohey and R. Hommel acknowledge support from the German
621 federal Ministry of Education (BMBF), research programmes "MiKlip"
622 (FKZ:01LP130A(CT):/01LP1130B(MT)), and ROMIC-ROSA (FKZ: 01LG1212A (RH)). C. Timmreck is also
623 supported by the European Union project StratoClim (FP7-ENV.2013.6.1-2). C. Brühl's PhD student S.
624 Schallock, who contributed to the compilation of the volcano inventory, is also supported by StratoClim. A.
625 Schmidt was funded by an Academic Research Fellowship from the School of Earth and Environment,
626 University of Leeds and NERC grant NE/N006038/1. M. Toohey acknowledges support by the Deutsche
627 Forschungsgemeinschaft (DFG) in the framework of the priority programme "Antarctic Research with
628 comparative investigations in Arctic ice areas" through grant TO 967/1-1. The National Center for Atmospheric
629 Research is funded by the National Science Foundation. Lindsay Lee is a Leverhulme Early Career Fellow
630 funded under the Leverhulme Trust grant ECF-2014-524.

631

632 **References**

- 633 Andres, R. J. and Kasgnoc, A. D.: A time-averaged inventory of subaerial volcanic sulfur emissions, J.
634 Geophys. Res., 103, 25251–25261, 1998.
- 635 Antuña, J. C., Robock, A., Stenchikov, G. L., Thomason, L. W. and Barnes, J. E.: Lidar validation of SAGE II
636 aerosol measurements after the 1991 Mount Pinatubo eruption, J. Geophys. Res., 107 (D14),
637 10.1029/2001JD001441, 2002.
- 638 Aquila, V., Oman, L. D., Stolarski, R. S., Colarco, P. R., and Newman, P. A.: Dispersion of the volcanic sulfate
639 cloud from a Mount Pinatubo-like eruption, J. Geophys. Res.-Atmos., 117, D06216,
640 doi:10.1029/2011JD016968, 2012.
- 641 Aquila, V., Oman, L. D., Stolarski, R., Douglass, A. R., and Newman, P. A.: The Response of Ozone and
642 Nitrogen Dioxide to the Eruption of Mt. Pinatubo at Southern and Northern Midlatitudes. Journal of
643 Atmospheric Science, 70(3), 894–900. doi:10.1175/JAS-D-12-0143.1, 2013.
- 644 Avdyushin, S.I. Tulinov, G. F., Ivanov, M. S., Kuzmenko, B. N., Mezhue, I. R., Nardi, B., Hauchecorne, I. A.,
645 Chanin, M.-L., 1. Spatial and temporal evolution of the optical thickness of the Pinatubo aerosol clouds in the
646 Northern Hemisphere from a network of ship-borne and stationary lidars, Geophys. Res. Lett., vol. 20, no. 18,
647 1963-1966, 1993.
- 648 Baran, A. J. and Foot, J. S.: New application of the operational sounder HIRS in determining a climatology of
649 sulphuric acid aerosol from the Pinatubo eruption, J. Geophys. Res., 99, 673–679, 1994.
- 650 Bekki, S.: Oxidation of volcanic SO₂: a sink for stratospheric OH and H₂O, Geophys. Res. Lett., 22, 913–916,
651 1995.
- 652 Bekki, S., Pyle, J. A., Zhong, Tourni, R., Haigh, J. D., and Pyle, D. M.: The role of microphysical and chemical
653 processes in prolonging the climate forcing of the Toba Eruption, Geophys. Res. Lett. 23, 2669–2672, 1996.
- 654 Bingen, C., Robert, C. E., Stebel, K., Brühl, C., Schallock, J., Vanhellefont, F., Mateshvili N., Höpfner, M.,
655 Trickl, T., Barnes, J.E., Jumelet, J., Vernier, J.-P., Popp T, Gerrit de Leeuw, G., Pinnock, S.: Stratospheric
656 aerosol data records for the climate change initiative: Development, validation and application to chemistry-
657 climate modelling. Remote Sensing of Environment. <https://doi.org/10.1016/j.rse.2017.06.002>, 2017
- 658 Bourassa, A. E., Degenstein, D. A., Gattinger, R. L., and Llewellyn, E. J.: Stratospheric aerosol retrieval with
659 OSIRIS limb scatter measurements, J. Geophys. Res., 112, D10 217, doi:10.1029/2006JD008079, 2007.
- 660 Bourassa, A. E., Robock, A., Randel, W. J., Deshler, T., Rieger, L. A., Lloyd, N. D., Llewellyn, E. J. T., and
661 Degenstein, D. A.: Large volcanic aerosol load in the stratosphere linked to Asian monsoon transport, Science,
662 337, 78–81, doi:10.1126/science.1219371, 2012.
- 663 Bovensmann, H. Burrows, J.P.; Buchwitz, M., Frerick, J., Noël, S., Rozanov, V. V., Chance, K.V., and Goede,
664 A. P. H : SCIAMACHY: Mission Objectives and Measurement Modes, J. Atmos. Sci., 56, 127–150, doi:
665 10.1175/1520-0469, 1999.



- 666 Browell, E. V., Butler, C. F., Fenn, M. A., Grant, W. B., Ismail, S., Schoeberl, M. R., Toon, O. B., Loewenstein,
667 M., Podolske, J. R.: Ozone and Aerosol Changes During the 1991-2 Airborne Arctic Stratospheric Expedition,
668 *Science*, 261, 1151-1158, 1993
- 669 Brühl, C., Lelieveld, J., Crutzen, P. J., and Tost, H.: The role of carbonyl sulphide as a source of stratospheric
670 sulphate aerosol and its impact on climate, *Atmos. Chem. Phys.*, 12, 1239–1253, doi:10.5194/acp-12-1239-
671 2012, 2012.
- 672 Brühl, C., Lelieveld, J., Tost, H., Höpfner, M., and Glatthor, N.: Stratospheric sulphur and its implications for
673 radiative forcing simulated by the chemistry climate model EMAC, *J. Geophys. Res.-Atmos.*, 120, 2103–2118,
674 doi:10.1002/2014JD022430, 2015.
- 675 Carn, S.A., Clarisse, L., and Prata, A. J.: Multi-decadal satellite measurements of global volcanic degassing, *J.*
676 *of Volcanology and Geothermal Research*, 311, 99-134, 2016.
- 677 Clemesha, B. R., Kent, G. S. and Wright, R. W. H.: Laser probing the lower atmosphere, *Nature*, vol. 209, 184-
678 185, 1966.
- 679 Crowley, T. J. and Unterman, M. B.: Technical details concerning development of a 1200 yr proxy index for
680 global volcanism, *Earth Syst. Sci. Data*, 5, 187–197, doi:10.5194/essd-5-187-2013, 2013.
- 681 Dee, D. P., Uppala, S. M., Simmons, A. J., Berrisford, P., Poli, P., Kobayashi, S., Andrae, U., Balmaseda, M.
682 A., Balsamo, G., Bauer, P., Bechtold, P., Beljaars, A. C. M., van de Berg, L., Bidlot, J., Bormann, N., Delsol,
683 C., Dragani, R., Fuentes, M., Geer, A. J., Haimberger, L., Healy, S. B., Hersbach, H., Holm, E. V., Isaksen, L.,
684 Kallberg, P., Kohler, M., Matricardi, M., McNally, A. P., Monge-Sanz, B. M., Morcrette, J. J., Park, B. K.,
685 Peubey, C., de Rosnay, P., Tavolato, C., Thepaut, J. N., and Vitart, F.: The ERA-Interim reanalysis:
686 Configuration and performance of the data assimilation system, *Q. J. R. Meteorol. Soc.*, 137, 553–597,
687 doi:10.1002/qj.828, 2011.
- 688 Dentener, F., Kinne, S., Bond, T., Boucher, O., Cofala, J., Generoso, S., Ginoux, P., Gong, S., Hoelzemann, J.
689 J., Ito, A., Marelli, L., Penner, J. E., Putaud, J.-P., Textor, C., Schulz, M., van der Werf, G. R., and Wilson, J.:
690 Emissions of primary aerosol and precursor gases in the years 2000 and 1750 prescribed data-sets for AeroCom,
691 *Atmos. Chem. Phys.*, 6, 4321-4344, doi:10.5194/acp-6-4321-2006, 2006.
- 692 Deshler, T.: In situ measurements of Pinatubo aerosol over Kiruna on four days between 18 January and 13
693 February 1992, *Geophys. Res. Lett.*, 21, 1323–1326, 1994
- 694 Deshler, T., Hervig, M. E., Hofmann, D. J., Rosen, J. M., and Liley, J. B.: Thirty years of in situ stratospheric
695 aerosol size distribution measurements from Laramie, Wyoming (41N), using balloon-borne instruments, *J.*
696 *Geophys. Res.-Atmos.*, 108, 4167 doi:10.1029/2002JD002514, 2003.
- 697 Deshler, T.: A review of global stratospheric aerosol: measurements, importance, life cycle, and local
698 stratospheric aerosol, *Atmos. Res.*, 90, 223–232, doi:10.1016/j.atmosres.2008.03.016, 2008.
- 699 Dhomse, S. S., Emmerson, K. M., Mann, G. W., Bellouin, N., Carslaw, K. S., Chipperfield, M. P., Hommel, R.,
700 Abraham, N. L., Telford, P., Braesicke, P., Dalvi, M., Johnson, C. E., O'Connor, F., Morgenstern, O., Pyle, J. A.,
701 Deshler, T., Zawodny, J. M., and Thomason, L. W.: Aerosol microphysics simulations of the Mt. Pinatubo



- 702 eruption with the UM-UKCA composition-climate model, *Atmos. Chem. Phys.*, 14, 11221–11246, doi:
703 10.5194/acp-14-11221-2014, 2014
- 704 Diehl, T., Heil, A., Chin, M., Pan, X., Streets, D., Schultz, M., and Kinne, S.: Anthropogenic, biomass burning,
705 and volcanic emissions of black carbon, organic carbon, and SO₂ from 1980 to 2010 for hindcast model
706 experiments, *Atmos. Chem. Phys. Discuss.*, 12, 24895–24954, doi:10.5194/acpd-12-24895-2012, 2012.
- 707 Dyer, A. J. and Hicks, B. B.: Stratospheric transport of volcanic dust inferred from surface radiation
708 measurements, *Nature*, no. 5006, 131-133, 1965.
- 709 Dyer, A. J. and Hicks, B. B.: Global spread of volcanic dust from the Bali eruption of 1963, *Q. J. Roy. Met.*
710 *Soc.*, 94, 545-554, 1968.
- 711 Ebert, M., Weigel, R., Kandler, K., Günther, G., Molleker, S., Groß, J.-U., Vogel, B., Weinbruch, S., and
712 Borrmann, S.: Chemical analysis of refractory stratospheric aerosol particles collected within the arctic vortex
713 and inside polar stratospheric clouds, *Atmos. Chem. Phys.*, 16, 8405-8421, [https://doi.org/10.5194/acp-16-8405-](https://doi.org/10.5194/acp-16-8405-2016)
714 2016, 2016.
- 715 Elterman, L. Wexler, R. and Chang, D. T.: Features of Tropospheric and Stratospheric Dust, *Applied Optics*,
716 vol. 8, No. 5, 893—903, 1969.
- 717 English, J. M., Toon, O. B., Mills, M. J., and Yu, F.: Microphysical simulations of new particle formation in the
718 upper troposphere and lower stratosphere, *Atmos. Chem. Phys.*, 11, 9303–9322, doi:10.5194/acp-11-9303-2011,
719 2011.
- 720 English, J. M., Toon, O. B. and Mills, M J: Microphysical simulations of large volcanic eruptions: Pinatubo and
721 Toba, *J. Geophys. Res. Atmos.*, 118, 1880–1895, doi:10.1002/jgrd.50196, 2013
- 722 Eyring, V., Lamarque, J.-F., Hess, P., Arfeuille, F., Bowman, K., Chipperfield, M. P., Duncan, B., Fiore, A.,
723 Gettelman, A., Giorgetta, M. A., Granier, C., Hegglin, M., Kinnison, D., Kunze, M., Langematz, U., Luo, B.,
724 Martin, R., Matthes, K., Newman, P. A., Peter, T., Robock, A., Ryerson, T., Saiz-Lopez, A., Salawitch, R.,
725 Schultz, M., Shepherd, T. G., Shindell, D., Staehelin, J., Tegtmeier, S., Thomason, L., Tilmes, S., Vernier, J.-P.,
726 Waugh, D. W., and Young, P. J.: Overview of IGAC/SPARC Chemistry-Climate Model Initiative (CCMI)
727 Community Simulations in Support of Upcoming Ozone and Climate Assessments, *SPARC Newsletter No. 40*,
728 p. 48-66, 2013
- 729 Flowers, E. C. and Viebrock, H. J.: Solar Radiation: An Anomalous Decrease of Direct Solar Radiation,
730 *Science*, 148 (3669), 493-494. 1965.
- 731 Friend, J. P.: Properties of the stratospheric aerosol, *Tellus*, 18, 465-473, 1966.
- 732 Gao, C., Oman, L., Robock, A. and Stenchikov, G. L.: Atmospheric volcanic loading derived from bipolar ice
733 cores: Accounting for the spatial distribution of volcanic deposition, *J. Geophys. Res.*, 112(D9),
734 doi:10.1029/2006JD007461, 2007.
- 735 Gao, C., Robock, A., and Ammann, C.: Volcanic forcing of climate over the past 1500 years: an improved ice
736 core-based index for climate models, *J. Geophys. Res.*, 113, D23111, doi:10.1029/2008JD010239, 2008.



- 737 Glatthor, N., Höpfner, M.; Baker, I. T.; Berry, J.; Campbell, J. E., Kawa, S. R., Krysztofiak, G. Leyser, A.,
738 Sinnhuber, B.-M. Stiller, G. P., Stinecipher, J. and von Clarmann, T.: Tropical sources and sinks of carbonyl
739 sulfide observed from space, *Geophys. Res. Lett.*, 42, 10,082–10,090, doi:10.1002/2015GL066293, 2015.
- 740 Grams, G. and Fiocco, G.: Stratospheric Aerosol Layer during 1964 and 1965, *J. Geophys. Res.*, 72(14), 3523-
741 3542, 1967.
- 742 Grainger, R. G., Lambert, A., Taylor, F. W., Remedios, J. J., Rogers, C. D., and Corney, M.: Infrared absorption
743 by volcanic stratospheric aerosols observed by ISAMS, *Geophys. Res. Lett.*, 20, 1287–1290, 1993.
- 744 Granier, C., Bessagnet, B., Bond, T. C., D'Angiola, A., Denier van der Gon, H., Frost, G. J., Heil, A., Kaiser, J.
745 W., Kinne, S., Klimont, Z., Kloster, S., Lamarque, J.-F., Liousse, C., Masui, T., Meleux, F., Mieville, A., Ohara,
746 T., Raut, J.-C., Riahi, K., Schultz, M. G., Smith, S. J., Thompson, A., Aardenne, J., Werf, G. R., and Vuuren, D.
747 P.: Evolution of anthropogenic and biomass burning emissions of air pollutants at global and regional scales
748 during the 1980-2010 period. *Climatic Change*, 109, 163-190, DOI: 10.1007/s10584-011-0154-1, 2011.
- 749 Guo, S., Bluth, G. J. S., Rose, W. I., Watson, I. M. and Prata, A. J.: Re-evaluation of SO₂ release of the 15 June
750 1991 Pinatubo eruption using ultraviolet and infrared satellite sensors, *Geochemistry Geophysics Geosystems*,
751 5(4), 1-31, 2004a.
- 752 Guo, S, Rose, W.I., Bluth, G.J.S: and Watson, I. M.: Particles in the great Pinatubo volcanic cloud of June 1991:
753 the role of ice, *Geochemistry, Geophysics, Geosystems*, 5, (5) Q05003, doi: 10.1029/2003GC000655, 2004b.
- 754 Hamill, P., Jensen, E. J., Russel, P. B., and Bauman, J. J.: The life cycle of stratospheric aerosol particles, *B.*
755 *Am. Meteorol. Soc.*, 78, 1395–1410, 1997.
- 756 Hamill, P. and Brogniez, C.: Ch 4. Stratospheric aerosol record and climatology, in: *SPARC Assessment of*
757 *Stratospheric Aerosol Properties*, edited by: Thomason, L. and Peter, T., World Climate Research Program 124,
758 Toronto, 107–176, 2006.
- 759 Hofmann, D. J. and Rosen, J. M.: Sulfuric acid droplet formation and growth in the stratosphere after the 1982
760 eruption of El Chichón, *Geophys. Res. Lett.*, 10, 313–316. doi:10.1029/GL010i004p00313, 1983.
- 761 Hofmann, D. J. and Rosen, J. M., On the prolonged lifetime of the El Chichón sulfuric acid aerosol cloud, *J.*
762 *Geophys. Res.*, 92(8), 9825–9830, 1987.
- 763 Hofmann, D., Barnes, J. O'Neill, M., Trudeau, M. and Neely, R.: Increase in background stratospheric aerosol
764 observed with lidar at Mauna Loa Observatory and Boulder, Colorado, *Geophys. Res. Lett.*, 36, 1–5, 2009.
- 765 Hommel, R., Timmreck, C., and Graf, H. F.: The global middle-atmosphere aerosol model MAECHAM5-
766 SAM2: comparison with satellite and in-situ observations, *Geosci. Model Dev.*, 4, 809–834, doi:10.5194/gmd-4-
767 809-2011, 2011.
- 768 Hommel, R., Timmreck, C., Giorgetta, M. A., and Graf, H. F.: Quasi-biennial oscillation of the tropical
769 stratospheric aerosol layer, *Atmos. Chem. Phys.*, 15, 5557-5584, doi:10.5194/acp-15-5557-2015, 2015.
- 770 Höpfner, M., Glatthor, N., Grabowski, U., Kellmann, S., Kiefer, M., Linden, A., Orphal, J., Stiller, G., von
771 Clarmann, T., Funke, B., and Boone, C. D.: Sulfur dioxide (SO₂) as observed by MIPAS/Envisat: temporal
772 development and spatial distribution at 15–45 km altitude, *Atmos. Chem. Phys.*, 13, 10405–10423,
773 doi:10.5194/acp-13-10405-2013, 2013.



- 774 Höpfner, M., Boone, C. D., Funke, B., Glatthor, N., Grabowski, U., Günther, A., Kellmann, S., Kiefer, M.,
775 Linden, A., Lossow, S., Pumphrey, H. C., Read, W. G., Roiger, A., Stiller, G., Schlager, H., von Clarmann, T.,
776 and Wissmüller, K.: Sulfur dioxide (SO₂) from MIPAS in the upper troposphere and lower stratosphere 2002–
777 2012, *Atmos. Chem. Phys.*, 15, 7017–7037, doi:10.5194/acp-15-7017-2015, 2015.
- 778 Jones, A. C., J. M. Haywood, A. Jones, and Aquila, V.: Sensitivity of volcanic aerosol dispersion to
779 meteorological conditions: A Pinatubo case study, *J. Geophys. Res. Atmos.*, 121, 6892 – 6908,
780 doi:10.1002/2016JD025001, 2016.
- 781 Kent, G. S., Clemesha, B. R and Wright, R. W.: High altitude atmospheric scattering of light from a laser beam,
782 *J. Atmos. Terr. Phys.*, vol. 29, 169–181, 1967.
- 783 Kinne, S., Toon, O.B., and Prather, M. J.: Buffering of stratospheric circulation by changing amounts of tropical
784 ozone a Pinatubo Case Study, *Geophys. Res. Lett.*, 19, 1927–1930, doi:10.1029/92GL01937, 1992.
- 785 Kokkola, H., Hommel, R., Kazil, J., Niemeier, U., Partanen, A.-I., Feichter, J., and Timmreck, C.: Aerosol
786 microphysics modules in the framework of the ECHAM5 climate model – intercomparison under stratospheric
787 conditions, *Geosci. Model Dev.*, 2, 97–112, doi:10.5194/gmd-2-97-2009, 2009.
- 788 Kovilakam, M., and Deshler T.: On the accuracy of stratospheric aerosol extinction derived from in situ size
789 distribution measurements and surface area density derived from remote SAGE II and HALOE extinction
790 measurements, *J. Geophys. Res. Atmos.*, 120, doi:10.1002/2015JD023303, 2015.
- 791 Kremser, S., Thomason, L. W., von Hobe, M., Hermann, M., Deshler, T., Timmreck, C., Toohey, M., Stenke,
792 A., Schwarz, J. P., Weigel, R., Fueglistaler, S., Prata, F. J., Vernier, J.-P., Schlager, H., Barnes, J. E., Antuña-
793 Marrero, J.-C., Fairlie, D., Palm, M., Mahieu, E., Notholt, J., Rex, M., Bingen, C., Vanhellefont, F., Bourassa,
794 A., Plane, J. M. C., Klocke, D., Carn, S. A., Clarisse, L., Trickl, T., Neely, R., James, A. D., Rieger, L., Wilson,
795 J. C. and Meland, B.: Stratospheric aerosol - Observations, processes, and impact on climate, *Rev. Geophys.*, 54,
796 doi:10.1002/2015RG000511, 2016.
- 797 Krueger, A. J., Krotkov, N. A., Carn, S. A: El Chichon: the genesis of volcanic sulfur dioxide monitoring from
798 space *J. Volcanol. Geotherm. Res.*, 175 (2008), pp. 408–414, 10.1016/j.jvolgeores.2008.02.026, 2008.
- 799 Lambert, A., Grainger, R., Remedios, J., Rodgers, C., Corney, M., and Taylor, F.: Measurements of the
800 evolution of the Mt. Pinatubo aerosol cloud by ISAMS, *Geophys. Res. Lett.*, 20, 1287–1290, 1993.
- 801 Lee, L. A., Carslaw, K. S., Pringle, K. J., Mann, G. W., and Spracklen, D. V.: Emulation of a complex global
802 aerosol model to quantify sensitivity to uncertain parameters, *Atmos. Chem. Phys.*, 11, 12253–12273,
803 doi:10.5194/acp-11-12253-2011, 2011.
- 804 Mann, G. W., Dhomse, S., Deshler, T., Timmreck, C., Schmidt, A., Neely, R. and Thomason, L.: Evolving
805 particle size is the key to improved volcanic forcings, *Past Global Change (PAGES)*, vol. 23, 2, 52–53, 2015.
- 806 Marshall, L., Schmidt, A., Toohey, M., Carslaw, K. S., Mann, G. W., Sigl, M., Khodri, M., Timmreck, C.,
807 Zanchettin, D., Ball, W., Bekki, S., Brooke, J. S. A., Dhomse, S., Johnson, C., Lamarque, J.-F., LeGrande, A.,
808 Mills, M. J., Niemeier, U., Poulain, V., Robock, A., Rozanov, E., Stenke, A., Sukhodolov, T., Tilmes, S.,
809 Tsigaridis, K., and Tummon, F.: Multi-model comparison of the volcanic sulfate deposition from the 1815
810 eruption of Mt. Tambora, *Atmos. Chem. Phys. Discuss.*, <https://doi.org/10.5194/acp-2017-729>, in review, 2017.



- 811 Mills, M. J., Schmidt, A., Easter, R., Solomon, S., Kinnison, D. E., Ghan, S. J., Neely III, R.R., Marsh, D R.;
812 Conley, A.; Bardeen, C.G. and Gettelman, A. Global volcanic aerosol properties derived from emissions, 1990–
813 2014, using CESM1(WACCM). *J. Geophys. Res.-Atmos.*, doi:10.1002/2015JD024290, 2016.
- 814 Montzka, S. A., Calvert, P., Hall, B. D., Elkins, J. W., Conway, T. J., Tans, P. P., and Sweeney, C.: On the
815 global distribution, seasonality, and budget of atmospheric carbonyl sulfide and some similarities with CO₂, *J.*
816 *Geophys. Res.*, 112, D09302, doi:10.1029/2006JD007665, 2007.
- 817 Moreno, H. and Stock, J.: The atmospheric extinction on Cerro Tololo during 1963, *Pub. Astron. Soc. Pacific*,
818 76, 55-56, 1964.
- 819 Mossop, S. C.: Stratospheric particles at 20km, *Nature*, 199, 325-326, 1963.
- 820 Mossop, S. C.: Volcanic dust collected at an altitude of 20km, *Nature*, 203, 824-827, 1964.
- 821 Myhre, G., Shindell, D., Bréon, F. M., Collins, W., Fuglestedt, J., Huang, J., Koch, D., Lamarque, J. F., Lee,
822 D., Mendoza, B., Nakajima, T., Robock, A., Stephens, G., Takemura, T., and Zhang, H.: Anthropogenic and
823 natural radiative forcing, in: *Climate Change 2013: The Physical Science Basis. Contribution of Working Group*
824 *I to the Fifth Assessment Report of the Intergovernmental Panel on Climate Change*, edited by: Stocker, T. F.,
825 Qin, D., Plattner, G.-K., Tignor, M., Allen, S. K., Nauels, A., Xia, Y., Bex, V., and Midgley, P. M., Cambridge
826 University Press, Cambridge, United Kingdom and New York, NY, USA, 2013.
- 827 Nardi, B., Chanin, M.-L., Hauchecorne, I. A., Avdyushin, S.I. Tulinov, G. F., Ivanov, M. S., Kuzmenko, B. N.,
828 Mezhue, I. R., *Geophys. Res. Lett.*, vol. 20, no. 18, 1967-1971, 1993.
- 829 National Research Council: *Climate Intervention: Reflecting Sunlight to Cool Earth*, The Natl. Acad. Press,
830 Washington, D. C, 2015.
- 831 Neely III, R. R., Toon, O. B., Solomon, S., Vernier, J. P., Alvarez, C., English, J. M., Rosenlof, K. H., Mills, M.,
832 Bardeen, C. G., Daniel, J. S., and Thayer, J. P.: Recent anthropogenic increases in SO₂ from Asia have minimal
833 impact on stratospheric aerosol, *Geophys. Res. Lett.*, 40, 999–1004, doi:10.1002/grl.50263, 2013.
- 834 Neely III, R. R., Yu, P., Rosenlof, K. H., Toon, O. B., Daniel, J. S., Solomon, S. and Miller, H. L.: The
835 contribution of anthropogenic SO₂ emissions to the Asian tropopause aerosol layer, *J. Geophys. Res. Atmos.*,
836 119, 1571–1579, doi:10.1002/2013JD020578, 2014.
- 837 Neely, R. and Schmidt, A.: *VolcanEESM: Global volcanic sulphur dioxide (SO₂) emissions database from 1850*
838 *to present -Version 1.0*, *Cent. Environ. Data Anal.*, doi:10.5285/76ebdc0b-0eed-4f70-b89e-55e606bcd568,
839 2016.
- 840 Niemeier, U., Timmreck, C., Graf, H.-F., Kinne, S., Rast, S., and Self, S.: Initial fate of fine ash and sulfur from
841 large volcanic eruptions, *Atmos. Chem. Phys.*, 9, 9043–9057, doi:10.5194/acp-9-9043-2009, 2009.
- 842 Niemeier, U. and Timmreck, C.: What is the limit of climate engineering by stratospheric injection of SO₂?
843 *Atmos. Chem. Phys.*, 15, 9129-9141, <https://doi.org/10.5194/acp-15-9129-2015>, 2015.
- 844 Oman, L., Robock, A., Stenchikov, G. L., Thordarson, T., Koch, D., Shindell, D. T., and Gao, C. C.: Modeling
845 the distribution of the volcanic aerosol cloud from the 1783-1784 Laki eruption, *J. Geophys. Res.-Atmos.*, 111,
846 D12209, doi:10.1029/2005JD006899, 2006



- 847 Pitari, G. and Mancini, E.: Short-term climatic impact of the 1991 volcanic eruption of Mt. Pinatubo and effects
848 on atmospheric tracers, *Natural Hazards and Earth System Science*, 2, 91–108, doi:10.5194/nhess-2-91-2002,
849 2002.
- 850 Pittock, A. B.: A thin stable layer of anomalous ozone and dust content, *J. Atmos. Sci.*, vol. 23, 538-542, 1966.
- 851 Plumb, R. A.: A “tropical pipe” model of stratospheric transport, *J. Geophys. Res.*, 101(D2), 3957–3972,
852 doi:10.1029/95JD03002, 1996.
- 853 Pueschel, R. F., Machta, L., Cotton, G. F., Flower, E. C., Peterson, J. T.: Normal Incidence Radiation Trends
854 and Mauna Loa, Hawaii, *Nature*, vol. 240, 545-547, 1972.
- 855 Pueschel, R. F., Russell, R. B., Allen, D. A., Ferry, G. V., Snetsinger, K. G., Livingston, J. M. and Verma, S.
856 Physical and optical properties of the Pinatubo volcanic aerosol: Aircraft observations with impactors and a
857 Sun-tracking photometer, *J. Geophys.*, vol. 99, no. D6, pp. 12,915-12,922, 1994
- 858 Rault, D. F., and Loughman, R. P.: The OMPS Limb Profiler Environmental Data Record Algorithm
859 Theoretical Basis Document and Expected Performance, *IEEE T. Geosci. Remote Sensing*, 51, 2505–2527,
860 doi:10.1109/TGRS.2012.2213093, 2013.
- 861 Rayner, N. A., D. E. Parker, E. B. Horton, C. K. Folland, L. V. Alexander, D. P. Rowell, E. C. Kent, and A.
862 Kaplan, Global analyses of sea surface temperature, sea ice, and night marine air temperature since the late
863 nineteenth century, *J. Geophys. Res.*, 108 14, 4407, doi:10.1029/2002JD002670, 2003.
- 864 Reeves, J. M., Wilson, J., Brock, C., A., and Bui, T.P.: Comparison of aerosol extinction coefficients, surface
865 area density, and volume density from SAGE II and in situ aircraft measurements, *J. Geophys. Res.*, 113,
866 D11202, doi:10.1029/2007JD009357, 2008.
- 867 Ridley, D. A., S. Solomon, S., Barnes, J.E., Burlakov, V.D., Deshler, T., Dolgii, S.I.; Herber, A.B., Nagai, T.
868 Neely III, R.R., Nevzorov, A. V., Ritter, C., Sakai, T., Santer, B. D., Sato, M., Schmidt, A., Uchino, O. and
869 Vernier, J.P.: Total volcanic stratospheric aerosol optical depths and implications for global climate change, *J.*
870 *Geophys. Res.*, 41, 7763-7769, doi:10.1002/2014GL061541, 2014.
- 871 Rieger, L. A., Bourassa, A. E, and Degenstein, D. A.: Merging the OSIRIS and SAGE II stratospheric aerosol
872 records, *J. Geophys. Res. Atmos.*, 120, doi:10.1002/2015JD023133, 2015.
- 873 Robock, A.: Volcanic eruptions and climate, *Rev Geophys*, 38, 191–219, doi:10.1029/1998RG000054, 2000.
- 874 Robock, A., MacMartin, D. G., Duren, R., and Christensen, M.W.: Studying geoengineering with natural and
875 anthropogenic analogs, *Climatic Change*, doi:10.1007/s10584-013-0777-5, published online, 2013.
- 876 Rollins, A. W., Thornberry, T. D., Watts, L.A., Yu, P., Rosenlof, K. H., Mills, M., Baumann, E., Giorgetta, F.R.,
877 Bui, T.V., Höpfner, M., Walker, K. A., Boone, C., Bernath, P. F., Colarco, P. R., Newman, P.A., Fahey, D.W.,
878 Gao, R.S.: The role of sulfur dioxide in stratospheric aerosol formation evaluated by using in situ measurements
879 in the tropical lower stratosphere, *Geophys. Res. Lett.*, 44, 4280–4286, doi:10.1002/2017GL072754, 2017.
- 880 Rougier, J., Sexton, D. M. H., Murphy, J. M. and Stainforth, D. A.: Analyzing the climate sensitivity of the
881 HadSM3 climate model using ensembles from different but related experiments, *J. Climate*, 22 (13). 3540-3557,
882 2009.
- 883 Rosen, J. M., The Vertical Distribution of Dust to 30 Kilometers, *J. Geophys. Res.*, 69 (21), 4673-4767, 1964.



- 884 Rosen, J. M., Correlation of dust and ozone in the stratosphere, *Nature*, 209, 1342, 1966
- 885 Rosen, J. M., Simultaneous Dust and Ozone Soundings over North and Central America, *J. Geophys. Res.*, vol.
- 886 73, no. 2, 479-486, 1968.
- 887 Russell, P. B., and McCormick, M. P.: SAGE II aerosol data validation and initial data use: An introduction and
- 888 overview, *J. Geophys. Res.*, 94, 8335–8338, 1989.
- 889 Santer, B. D., Bonfils, C., Painter, J. F., Zelinka, M. D., Mears, C., Solomon, S., Schmidt, G. A., Fyfe, J. C.,
- 890 Cole, J. N. S., Nazarenko, L., Taylor, K. E., and Wentz, F. J.: Volcanic contribution to decadal changes in
- 891 tropospheric temperature, *Nat. Geosci.*, 7, 185–189, doi:10.1038/ngeo2098, 2014.
- 892 Santer, B. D., Solomon, S.; Bonfils, C., Zelinka, M. D., Painter, J. F., Beltran, F., Fyfe, C., Johannesson, G.,
- 893 Mears, C., Ridley, D.A., Vernier, J.-P., and Wentz, F.J.: Observed multivariable signals of late 20th and early
- 894 21st century volcanic activity, *Geophys. Res. Lett.*, 42, 500–509, doi:10.1002/2014GL062366, 2015.
- 895 Self S., and King, A.J.: Petrology and sulfur and chlorine emissions of the 1963 eruption of Gunung Agung,
- 896 Bali, Indonesia. *Bull. Volcanol.* 58:263-285, 1996.
- 897 Sheng, J.-X., Weisenstein, D. K., Luo, B.-P., Rozanov, E., Stenke, A., Anet, J., Bingemer, H., and Peter, T.:
- 898 Global atmospheric sulfur budget under volcanically quiescent conditions: aerosol–chemistry–climate model
- 899 predictions and validation, *J. Geophys. Res.-Atmos.*, 120, 256–276, doi:10.1002/2014JD021985, 2015a
- 900 Sheng, J.-X., Weisenstein, D. K., Luo, B.-P., Rozanov, E., Arfeuille, F., and Peter, T.: A perturbed parameter
- 901 model ensemble to investigate 1991 Mt Pinatubo's initial sulfur mass emission, *Atmos. Chem. Phys.*, 15, 11501–
- 902 11512, doi:10.5194/acp-15-11501-11512, 2015b.
- 903 Sigl, M., Winstrup, M., McConnell, J. R., Welten, K. C., Plunkett, G., Ludlow, F., Büntgen, U., Caffee, M.,
- 904 Chellman, N., Dahl-Jensen, D., Fischer, H., Kipfstuhl, S., Kostick, C., Maselli, O. J., Mekhaldi, F., Mulvaney,
- 905 R., Muscheler, R., Pasteris, D. R., Pilcher, J. R., Salzer, M., Schüpbach, S., Steffensen, J. P., Vinther, B. M. and
- 906 Woodruff, T. E.: Timing and climate forcing of volcanic eruptions for the past 2,500 years, *Nature*, 523, 543–
- 907 549, doi:10.1038/nature14565, 2015.
- 908 Solomon, S., Daniel, J.S., Neely III, R.R., Vernier, J.P., Dutton, E.G: and Thomason, L.W.: The Persistently
- 909 Variable “Background” Stratospheric Aerosol Layer and Global Climate Change, *Science*, 866-870, 2011.
- 910 Solomon S, Ivy, DJ, Kinnison, D, Mills, MJ, Neely III, R.R, Schmidt, A. Emergence of healing in the Antarctic
- 911 ozone layer. *Science.*, doi: 10.1126/science.aae0061, 2016.
- 912 Stevens, T. D., Haris, P. A. T., Rau, Y.-C. and Philbrick, C. R., Latitudinal lidar mapping of stratospheric
- 913 particle layers, *Adv. Space Res.*, vol. 14, 9, 193–198, 1994.
- 914 Stoffel, M., Khodri, M., Corona, C., Guillet, S., Poulain, V., Bekki, S., Guiot, J., Luckman, B. H., Oppenheimer,
- 915 C., Lebas, N., Beniston, M. and Masson-Delmotte, V.: Estimates of volcanic- induced cooling in the Northern
- 916 Hemisphere over the past 1,500 years, *Nat. Geosci.*, 8, 784–788, doi:10.1038/ngeo2526, 2015.
- 917 Stothers, R. B. and Rampino, M. R.: Volcanic eruptions in the Mediterranean before A.D. 630 from written and
- 918 archaeological sources, *J. Geophys. Res.*, 88(B8), 6357, doi:10.1029/JB088iB08p06357, 1983.
- 919 Stothers, R. B.: Major optical depth perturbations to the stratosphere from volcanic eruptions: Pyrheliometric
- 920 period, 1881–1960, *J. Geophys. Res.*, 101(D2), 3901–3920, doi:10.1029/95JD03237, 1996.



- 921 Stothers, R.B.: Stratospheric aerosol clouds due to very large volcanic eruptions of the early twentieth century:
922 Effective particle sizes and conversion from pyr heliometric to visual optical depth, *J. Geophys. Res.*, 102, 6143-
923 6151, doi:10.1029/96JD03985, 1997.
- 924 Stothers, R. B.: Major optical depth perturbations to the stratosphere from volcanic eruptions: Stellar extinction
925 period, 1961–1978, *J. Geophys. Res.*, 106(D3), 2993–3003, doi:10.1029/2000JD900652, 2001.
- 926 Stothers, R. B.: Cloudy and clear stratospheres before A.D. 1000 inferred from written sources, *J. Geophys.*
927 *Res.*, 107(D23), 4718, doi:10.1029/2002JD002105, 2002.
- 928 SPARC: Assessment of Stratospheric Aerosol Properties (ASAP), SPARC Report No. 4, edited by: Thomason,
929 L. and Peter, T., World Climate Research Programme WCRP-124, WMO/TD No. 1295, 2006.
- 930 Telford, P. J., Braesicke, P., Morgenstern, O. and Pyle, J. A.: Technical Note: Description and assessment of a
931 nudged version of the new dynamics Unified Model, *Atmos. Chem. Phys.*, 8, 1701–1712, 2008
- 932 Thomason, L. W., Burton, S. P., Luo, B.-P., and Peter, T.: SAGE II measurements of stratospheric aerosol
933 properties at non-volcanic levels, *Atmos. Chem. Phys.*, 8, 983-995, doi:10.5194/acp-8-983-2008, 2008.
- 934 Thomason, L. W. and Vernier, J.-P.: Improved SAGE II cloud/aerosol categorization and observations of the
935 Asian tropopause aerosol layer: 1989–2005, *Atmos. Chem. Phys.*, 13, 4605-4616, doi:10.5194/acp-13-4605-
936 2013, 2013.
- 937 Timmreck, C., Graf, H.-F., and Feichter, J.: Simulation of Mt. Pinatubo volcanic aerosol with the Hamburg
938 Climate Model ECHAM4, *Theor. Appl. Climatol.*, 62, 85–108, doi:10.1007/s007040050076, 1999a.
- 939 Timmreck, C., Graf, H.-F., and I. Kirchner, I.: A one and a half year interactive simulation of Mt. Pinatubo
940 aerosol, *J. Geophys. Res.*, 104, 9337-9360, 1999b.
- 941 Timmreck, C., Graf, H.F., Lorenz, S.J., Niemeier, U., Zanchettin, D., Matei D., Jungclaus, J.H., Crowley, T.J. :
942 Aerosol size confines climate response to volcanic super-eruptions, *Geophys. Res. Lett.*, 37:L24705,
943 doi:10.1029/2010GL04546, 2010.
- 944 Timmreck, C.: Modeling the climatic effects of large explosive volcanic eruptions, *Wiley Interdisciplinary*
945 *Reviews: Climate Change*, 3, 545–564, doi:10.1002/wcc.192, 2012
- 946 Toohey, M., Krüger, K., Niemeier, U., and Timmreck, C.: The influence of eruption season on the global
947 aerosol evolution and radiative impact of tropical volcanic eruptions, *Atmos. Chem. Phys.*, 11, 12351–12367,
948 doi:10.5194/acp-11-12351-2011, 2011.
- 949 Toohey, M., Krüger, K. and Timmreck, C.: Volcanic sulfate deposition to Greenland and Antarctica: A
950 modeling sensitivity study, *J. Geophys. Res. Atmos.*, 118(10), 4788–4800, doi:10.1002/jgrd.50428, 2013.
- 951 Toohey, M., Krüger, K., Bittner, M., Timmreck, C. and Schmidt, H.: The impact of volcanic aerosol on the
952 Northern Hemisphere stratospheric polar vortex: mechanisms and sensitivity to forcing structure, *Atmos. Chem.*
953 *Phys.*, 14, 13063-13079, doi:10.5194/acp14-13063-2014, 2014.
- 954 Toohey, M., Krüger, K., Sigl, M., Stordal, F. and Svensen, H.: Climatic and societal impacts of a volcanic
955 double event at the dawn of the Middle Ages, *Clim. Change*, 136(3–4), 401–412, doi:10.1007/s10584-016-
956 1648-7, 2016a.



- 957 Toohey, M., Stevens, B., Schmidt, H., and Timmreck, C.: Easy Volcanic Aerosol (EVA v1.0): an idealized
958 forcing generator for climate simulations, *Geosci. Model Dev.*, 9, 4049–4070, doi:10.5194/gmd-9-4049-2016,
959 2016b.
- 960 Trepte C. R. and Hitchman, M. H.: Tropical stratospheric circulation deduced from satellite aerosol data,
961 *Nature*, 355, 626–628, 1992.
- 962 Vehkamäki, H., Kulmala, M., Napari, I., Lehtinen, K. E. J., Timmreck, C., Noppel, M., and Laaksonen, A.: An
963 improved parameterization for sulfuric acid-water nucleation rates for tropospheric and stratospheric conditions,
964 *J. Geophys. Res.*, 107(D22), AAC3.1–AAC3.10, doi:10.1029/2002JD002184, 2002.
- 965 Vernier, J. P., Pommereau, J.P., Garnier, A., Pelon, J., Larsen, N., Nielsen, J., Christensen, T., Cairo, F.,
966 Thomason, L. W., Leblanc, T. and McDermid, I. S.: Tropical stratospheric aerosol layer from CALIPSO lidar
967 observations, *J. Geophys. Res.*, 114, D00H10, doi:10.1029/2009JD011946, 2009.
- 968 Vernier, J.-P., L. W. Thomason, J. Kar, CALIPSO detection of an Asian tropopause aerosol layer, *Geophys.*
969 *Res. Lett.*, 38, L07804, doi:10.1029/2010GL046614, 2011a
- 970 Vernier, J.-P., Thomason, L. W., Pommereau, J.-P., Bourassa, A., Pelon, J., Garnier, A., Hauchecorne, A.,
971 Blanot, L., Trepte, C., Degenstein, D., and Vargas, F.: Major influence of tropical volcanic eruptions on the
972 stratospheric aerosol layer during the last decade, *Geophys. Res. Lett.*, 38, L12807, doi:10.1029/2011GL047563,
973 2011b.
- 974 Volz, F. E.: Twilight phenomena caused by the eruption of Agung volcano, *Science*, 144 (3622), 1121–1122.
975 1964.
- 976 Volz, F. E.: Note on the global variation of stratospheric turbidity since the eruption of Agung volcano, *Tellus*,
977 17, 513–515, 1965.
- 978 Volz, F. E.: Atmospheric Turbidity after the Agung Eruption of 1963 and Size Distribution of the Volcanic
979 Aerosol, *J. Geophys. Res.*, 75, 27, 5185–5193, 1970.
- 980 von Savigny, C., Ernst, F., Rozanov, A., Hommel, R., Eichmann, K.-U., Rozanov, V., Burrows, J. P., and
981 Thomason, L. W.: Improved stratospheric aerosol extinction profiles from SCIAMACHY: validation and
982 sample results, *Atmos. Meas. Tech.*, 8, 5223–5235, doi:10.5194/amtd-8-5223-2015, 2015.
- 983 Weisenstein, D. K., Penner, J. E., Herzog, M., and Liu, X.: Global 2-D intercomparison of sectional and modal
984 aerosol modules, *Atmos. Chem. Phys.*, 7, 2339–2355, doi:10.5194/acp-7-2339-2007, 2007.
- 985 Winker, D. M. and Osborn, M. T.: Airborne lidar observations of the Pinatubo volcanic plume, *Geophys. Res.*,
986 *Lett.*, vol. 19, 2, 167–170, 1992.
- 987 Young, R. E., Houben, H., and Toon, O. B.: Radiatively forced dispersion of the Mt. Pinatubo volcanic cloud
988 and induced temperature perturbations in the stratosphere during the first few months following the eruption,
989 *Geophys. Res. Lett.*, 21, 369–372, 1994.
- 990 Young, S. A., Manson, P. J. and Patterson, G. R.: Southern Hemisphere Lidar measurements of the Aerosol
991 Clouds from Mt Pinatubo and Mt Hudson, Extended Abstracts of the 16th International Laser Radar Conference,
992 July 1992, MIT, Cambridge, Massachusetts, 1994.



993 Yu, P., Toon, O. B., Neely, R. R., Martinsson, B. G., and Brenninkmeijer, C. A. M.: Composition and physical
994 properties of the Asian Tropopause Aerosol Layer and the North American Tropospheric Aerosol Layer.
995 *Geophys. Res. Lett.*, 42(7), 2540–2546, doi: 10.1002/2015GL063181, 2015.

996 Yorks, J. E., Palm, S. P. McGill, M. J. Hlavka, D. L. Hart, W. D., Selmer, P. A., and Nowottnick, E. P.: CATS
997 Algorithm Theoretical Basis Document, 1st ed., NASA, 2015.

998 Zanchettin, D., Timmreck, C., Graf, H.-F., Rubino, A., Lorenz, S., Lohmann, K., Krueger, K., and Jungclaus, J.
999 H.: Bi-decadal variability excited in the coupled ocean–atmosphere system by strong tropical volcanic eruptions,
1000 *Clim. Dynam.*, 39, 419–444, doi:10.1007/s00382-011-1167-1, 2012.

1001 Zanchettin, D., Khodri, M., Timmreck, C., Toohey, M., Schmidt, A., Gerber, E. P., Hegerl, G., Robock, A.,
1002 Pausata, F. S. R., Ball, W. T., Bauer, S. E., Bekki, S., Dhomse, S. S., LeGrande, A. N., Mann, G. W., Marshall,
1003 L., Mills, M., Marchand, M., Niemeier, U., Poulain, V., Rozanov, E., Rubino, A., Stenke, A., Tsigaridis, K., and
1004 Tummon, F.: The Model Intercomparison Project on the climatic response to Volcanic forcing (VolMIP):
1005 experimental design and forcing input data for CMIP6, *Geosci. Model Dev.*, 9, 2701–2719, doi:10.5194/gmd-9-
1006 2701-2016, 2016.

1007



1008 **Tables**

Experiment	Focus	Number of specific experiments	Years per experiment	Total years^A	Knowledge-gap to be addressed
Background Stratospheric Aerosol [BG]	Stratospheric sulphur budget in volcanically quiescent conditions	1 mandatory + 2 recommended	20	20(60)	20 year climatology to understand sources and sinks of stratospheric background aerosol, assessment of sulfate aerosol load under volcanically quiescent conditions
Transient Aerosol Record [TAR]	Transient stratospheric aerosol properties over the period 1998 to 2012 using different volcanic emission datasets	4 mandatory +3 optional experiments recommended are 5 (see also Table 4)	15	60 (75,105)	Evaluate models over the period 1998-2012 with different volcanic emission data sets Understand drivers and mechanisms for observed stratospheric aerosol changes since 1998
Historic Eruption SO₂ Emission Assessment [HErSEA]	Perturbation to stratospheric aerosol from SO ₂ emission appropriate for 1991 Pinatubo, 1982 El Chichón, 1963, Agung	for each (x3) eruption (Control, median and 4 (2x2) of hi/lo deep/shallow (see also Table 6)	4 recom. 6	180 (270)	Assess how injected SO ₂ propagates through to radiative effects for different historical major tropical eruptions in the different interactive stratospheric aerosol models Use stratospheric aerosol measurements to constrain uncertainties in emissions and gain new observationally-constrained volcanic forcing and surface area density datasets Explore the relationship between volcanic emission uncertainties and volcanic forcing uncertainties
Pinatubo Emulation in Multiple Models [PoEMS]^B	Perturbed parameter ensemble of runs to quantify uncertainty in each model's predictions	Each model to vary , 5 or 3 of 8 parameters (7 per parameter = 56 35 or 21)	5 per parameter	280, 175 or 105 (8, 5 or 3)	Intercompare Pinatubo perturbation to strat- aerosol properties with full uncertainty analysis over PPE run by each model. Quantify sensitivity of predicted Pinatubo perturbation stratospheric aerosol properties and radiative effects to uncertainties in injection settings and model processes Quantify and intercompare sources of uncertainty in simulated Pinatubo radiative forcing for the different complexity models.

1009 ^A Each model will need to include an appropriate initialization and spin-up time for each ensemble member (~3-6 years depending on model
1010 configuration).

1011 ^B Note, that we are aware that some of the structural parameter variations in PoEMS will introduce some inherent drift in stratospheric
1012 aerosol properties for the background control run. However, initial test runs suggest the effect will be much larger for the volcanic
1013 perturbation. We therefore expect the effect of the control-drift on derived radiative forcings to be small. Models running tropospheric and
1014 stratospheric aerosol interactively will need to restrict the parameter scaling to the stratosphere.
1015

1016 **Table 1 General overview of the SSIRC ISA-MIP experiments.**

1017



Measurement/Platform	Time period 1998-2014	Reference
SO ₂ profile/MLS	2004-2011	Pumphrey et al., 2015
SO ₂ profile/MIPAS	2002-2012	Höpfner et al., 2013; 2015
Aerosol extinction profile, size/SAGE II	1998-2005	Russell and McCormick, 1989
Aerosol extinction profile, size/OSIRIS	2001-2011	McLinden et al., 2012; Rieger et al., 2015
Aerosol extinction profile/GOMOS	2002-2021	Vanhellemont et al., 2010
Aerosol extinction profile/SCIAMACHY	2002-2012	Taha et al., 2011; von Savigny et al. 2015
Aerosol extinction profile/CALIOP	2006-2011	Vernier et al., 2009, 2011a,b
Aerosol extinction or AOD merged products	1998-2011	Rieger et al., 2015
AOD from AERONET and lidars		Ridley et al., 2014
Surface area density		Kovilakam and Deshler, 2015 Eyring et al. (2013)

1018

1019 **Table 2: List of stratospheric aerosol and SO₂ observations available for the BG and TAR time period.**

1020

<u>Exp- Name</u>	<u>Specific description / Volcanic emission</u>	<u>Period</u>	<u>Ensemble Size</u>	<u>Years per member</u>	<u>Tier</u>
BG_QBO	Background simulation	Time slice year-2000 monthly-varying with internal or nudged QBO	1	20	1
BG_NQBO	Perpetual easterly phase of the QBO for the whole simulation	Time slice year-2000 monthly varying without QBO	1	20	2
BG_NAT	Only natural sources of aerosol (including biomass burning)	Time slice year-2000 monthly varying with internal of nudged QBO (when possible)	1	20	2

1021

1022 **Table 3: Overview of BG experiments.**

1023

1024



Volcanic Database	VolcDB1	VolcDB2	VolcDB3	VolcDB4	VolcDBSUB	VolcDB1_3D
Covering period	Dec/1997 - Apr/2012	Jan/1990 - Dec/2014	1978-2014	1979-2010		Dec/1997- Apr/2012
Observational data sets	MIPAS., GOMOS, SAGEII, TOMS, OMI	OMI, OMPS, IASI, TOMS, GOME/2., AIRS, MLS, MIPAS	TOMS, HIRS/2, AIRS, OMI, MLS, IASI and OMPS	TOMS, OMI		MIPAS., GOMOS, SAGEII, TOMS, OMI
Reference	Brühl et al. (2015), Bingen et al. (2017), Table S6	Mills et al. (2016, Neely and Schmidt (2016))	Carn et al. (2016)	Diehl et al., (2012), AeroCom-II HCA0 v1/v2, http://aerocom.met.no/emissions.html	Subset of 8 volcanoes Contains SO ₂ emissions and plume altitudes averaged over the 3 mandatory databases, details are given in the appendix.	3D netCDF Brühl et al. (2015), Bingen et al. (2017), Table S.6

1025

1026 **Table 4: Overview of volcanic emission data sets for the different TAR experiments. Sensor acronyms: (MIPAS:**
 1027 **Michelson Interferometer for Passive Atmospheric Sounding; GOMOS: Global Ozone Monitoring by Occultation of**
 1028 **Stars TOMS: Total Ozone Mapping Spectrometer; OMI: Ozone Monitoring Instrument; OMPS: Ozone Mapping**
 1029 **and Profiler Suite; IASI: Infrared Atmospheric Sounding Interferometer; GOME: Global Ozone Monitoring**
 1030 **Experiment; AIRS: Atmospheric Infrared Sounder; MLS: Microwave Limb Sounder; HIRS: High-resolution**
 1031 **Infrared Radiation Sounder; (References to the observational data and emission sources included are given in the**
 1032 **reference paper and for VolcDB1_3D also in Table S2.1. VolcDB1_3D is a three-dimensional database, containing**
 1033 **the spatial distributions of the injected SO₂ as initially observed by the satellite instruments. In both versions of**
 1034 **VolcDB1, the integral SO₂ mass of each injection is consistent.**
 1035

1036

1037



<u>Exp- Name</u>	<u>Volcanic Database Name</u>	<u>Specific description</u>	<u>Period</u>	<u>Years per member</u>	<u>TiER</u>
TAR_base	--	No sporadically erupting volcanic emission	Transient 1998-2012 monthly-varying	15	1
TAR_db1	VolcDB1	Volcanic emission data set (Bruehl et al., 2015 and updates)	Transient 1998-2012 monthly-varying	15	1
TAR_db2	VolcDB2	Volcanic emission data set (Mills et al. 2016)	Transient 1998-2012 monthly-varying	15	1
TAR_db3	VolcDB3	Volcanic emission data set (Carn et al. 2016)	Transient 1998-2012 time-varying	15	1
TAR_db4	VolcDB4	Volcanic emission data set (Diehl et al. 2012) and updates	Transient 1998-2010 time-varying	13	3
TAR_sub	VolcDBSUB	subset of strongest 8 volcanoes; averaged SO ₂ emissions and averaged injection heights from VolcDB1/2/3	Transient 1998-2012 monthly-varying	15	2
TAR_db1_3D	VolcDB1_3D	netCDF version of volcanic emission data set VolcDB1 (Bruehl et al., 2015 and updates)	Transient 1998-2012 monthly-varying	15	3

1038

1039 **Table 5: Overview of TAR experiments.**

1040



1041

<u>Exp- Name</u>	<u>Specific description / Volcanic emission</u>	<u>Period</u>	<u>Ensemble Size</u>	<u>Years per member</u>	<u>TiER</u>
HErSEA_Pin_Em_Ism	<u>Pinatubo episode</u> , SO ₂ Emission = medium, Inject shallow @medium-alt.	Transient 1991-1995 incl. GHGs & ODSs (monthly-varying SST & sea-ice from HadISST as for CCMI)	3	5	1
HErSEA_Pin_Eh_Ism	<u>Pinatubo episode</u> , SO ₂ Emission = high, Inject shallow @medium-alt.		3	5	1
HErSEA_Pin_El_Ism	<u>Pinatubo episode</u> , SO ₂ Emission = low, Inject shallow @medium-alt		3	5	1
HErSEA_Pin_Em_Isl	<u>Pinatubo episode</u> , SO ₂ Emission = medium, Inject shallow @low-alt		3	5	2
HErSEA_Pin_Em_Idp	<u>Pinatubo episode</u> , SO ₂ Emission= medium, Inject over deep altitude-range		3	5	2
HErSEA_Pin_Cntrol	<u>Pinatubo episode</u> , No Pinatubo SO ₂ emission		3	5	1
HErSEA_EIC_Em_Ism	<u>El Chichón episode</u> , SO ₂ Emission= medium, Inject shallow@ medium-alt	Transient 1982-1986 incl. GHGs & ODSs (monthly-varying SST and sea-ice from HadISST as for CCMI)	3	5	1
HErSEA_EIC_Eh_Ism	<u>El Chichón episode</u> , SO ₂ Emission= high, Inject shallow@medium-alt		3	5	1
HErSEA_EIC_El_Ism	<u>El Chichón episode</u> , SO ₂ Emission = low, Inject shallow@medium-alt		3	5	1
HErSEA_EIC_Em_Isl	<u>El Chichón episode</u> , SO ₂ Emission=medium, Inject shallow@low-altitude		3	5	2
HErSEA_EIC_Em_Idp	<u>El Chichón episode</u> , SO ₂ Emission= medium, Inject over deep altitude-range		3	5	2
HErSEA_EIC_Cntrol	<u>El Chichón episode</u> no El Chichón SO ₂ emission		3	5	1
HErSEA_Agg_Em_Ism	<u>Agung episode</u> SO ₂ Emission= medium, Inject shallow @medium-alt	Transient 1963-1967 incl. GHGs & ODSs(monthly-varying SST and sea-ice from HadISST as for CCMI)	3	5	1
HErSEA_Agg_Eh_Ism	<u>Agung episode</u> , SO ₂ Emission= high, Inject shallow @medium-alt		3	5	1
HErSEA_Agg_El_Ism	<u>Agung episode</u> , SO ₂ Emission = low, Inject shallow @medium-alt		3	5	1
HErSEA_Agg_Em_Isl	<u>Agung episode</u> , SO ₂ Emission = medium, Inject shallow @low-alt		3	5	2
HErSEA_Agg_Em_Idp	<u>Agung episode</u> , SO ₂ Emission =medium, Inject over deep altitude-range		3	5	2
HErSEA_Agg_Cntrol	<u>Agung episode</u> no Agung SO ₂ emission		3	5	1

1042 **Table 6: Overview of HErSEA experiments**



1043

Eruption	Measurement/platform	References
Pinatubo	Extinction/AOD [multi-l]: SAGE-II, AVHRR, HALOE, CLAES Balloon-borne size-resolved concentration profiles (CPC, OPC) Impactors on ER2 (AASE2), FCAS and FSSP on ER2 (AASE2) Ground-based lidar; airborne lidar Ship-borne lidar measurements	Hamill and Brogniez (SPARC, 2006, and references therein) Deshler et al (1994, Kiruna, EASOE), Deshler et al. (2003) Pueschel et al. (1994), Wilson et al. (1993), Brock et al. (1993) NDACC archive; Young, S. A et al. (1994), Browell et al., (1993) Avdyushin et al. (1993); Nardi et al. (1993), Stevens et al. (1994)
El-Chichón	Satellite extinction/AOD 1000nm (SAM-II) Balloon-borne particle concentration profiles Ground-based lidar	Hamill and Brogniez (SPARC, 2006 & references therein) Hofmann and Rosen (1983; 1987). NDACC archive
Agung	Surface radiation measurements (global dataset gathered in Dyer and Hicks; 1968) Balloon-borne measurements Ground-based lidar, searchlight and twilight measurements Aircraft measurements	Dyer and Hicks (1965), Pueschel et al. (1972), Moreno and Stock (1964), Flowers and Viebrock (1965) Rosen (1964; 1966, 1968), Pittock (1966) Clemesha et al. (1966), Grams & Fiocco (1967), Kent et al. (1967) Elterman et al., (1969), Volz (1964; 1965; 1970) Mossop et al. (1963; 1964), Friend (1966)

1044

1045

1046

1047

1048

1049

Table 7 List of stratospheric aerosol observation datasets from the 3 large eruptions of the 21st century (Agung, El Chichón and Mt. Pinatubo). For NDACC archive, see <http://www.ndsc.ncep.noaa.gov/data/>

Eruption	Location	Date	SO ₂ (Tg)	Shallow x 2	Deep
Mt. Pinatubo	15°N, 120°E	15/06/1991	10-20 (14)	18-20, 21-23km	18-25km
El Chichón	17°N, 93°W	04/04/1982	5-10 (7)	22-24, 24-26km	22-27km
Mt. Agung	8°S, 115°E	17/03/1963	5-10 (7)	17-19, 20-22km	17-23km

1050

1051

1052

1053

1054

1055

1056

1057

1058

1059

1060

1061

1062

1063

1064

1065

1066

Table 8: Settings to use for initialising the mini-ensemble of interactive stratospheric aerosol simulations for each eruption in the HERSEA experiment. For Pinatubo the upper range of SO₂ emission is based on TOMS/TOVS SO₂ observations (Guo et al., 2004a). The SO₂ emissions flux ranges and central-values (in parentheses) are specifically for application in interactive stratospheric aerosol (ISA) models, rather than any new data compilation. The lower range and the central values according to some recent Pinatubo studies (Dhomse et al., 2014; Mills et al., 2016; Sheng et al., 2015a) which have identified a modest downward-adjustment of initial observed SO₂ amounts to agree to HIRS/ISAMS measurements of peak sulphate aerosol loading (Baran and Foot, 1994). The adjustment assumes either uncertainties in the satellite measurements or that loss pathways in the first few weeks after these eruptions are either underpredicted (e.g. due to coarse spatial resolution) or omitted completely (accommodation onto ash/ice) in the ISA models. The El Chichón SO₂ central estimate is taken from Krueger et al. (2008), and an emission range based on assumed ±33% while for Agung the SO₂ emission estimate is from Self and King (1996). For Pinatubo, injection height-ranges for the two shallow and one deep realisation are taken from Antuña et al. (2002). The El Chichón values are based on the tropical lidar signal from Figure 4.34 of Hamill and Brogniez (2006), whereas for Agung we considered the measurements presented in Dyer and Hicks (1968) including balloon soundings (Rosen, 1964) and ground-based lidar (Grams and Fiocco, 1967).



1067

SO ₂ mass (Tg S)	Study	SO ₂ Height (km)
5	Dhomse et al., 2014	19-27
5	Mills et al. (2016)	18-20
7	Sheng et al. (2015a;b)	17-30
8.5	Timmreck et al. (1999a;b)	20-27
8.5	Niemeier et al. (2009); Toohey et al. (2011)	24
8.5	Brühl et al., (2015)	18-26*
10	Pitari and Mancini (2002)	18-25
10	Oman et al. (2006)	19-29
10	Aquila et al. (2012; 2013)	16-18, 17-27
10	English et al. (2013)	15.1-28.5

1068

1069 **Table 9: List of SO₂ injection settings used in different interactive stratospheric aerosol model simulations of the 1991**
 1070 **Mount Pinatubo eruption. * main peak at 23.5km, secondary peak at 21km.**

1071



1072

1073

	Parameters	Minimum set	Reduced set	Standard set	Uncertainty range
1	Injected SO ₂ mass	X	X	X	5 Tg-S – 10 Tg-S
2	Mid-point height of 3km-thick injection	X	X	X	18km – 30km
3	Latitudinal extent of the injection	X	X	X	Factor 0-1 to vary from 1-box injection at 15N (factor=0) to equator-to-15N (factor=1) *
4	Sedimentation velocity		X	X	Multiply model calculated velocity by a factor 0.5 to 2.
5	SO ₂ oxidation scaling		X	X	Scale gas phase oxidation of SO ₂ by a factor 0.5 to 2
6	Nucleation rate of sulfate particles			X	Scale model calculated rate by a factor 0.5 to 2.
7	Sub-grid particle formation factor.			X	Emit fraction of SO ₂ as sulphuric acid particles formed at sub-grid-scale (0 to 10%)
8	Coagulation rate			X	Scale the model calculated rate by a factor 0.5 to 2.

1074

1075

1076

1077

1078

1079

Table 10: Groups will need to translate the 0-1 latitude-spread parameter into a sequence of fractional injections into all grid boxes between the equator and 15 °N. For example for a model with 2.5 degree latitude resolution, the relative injection in the 6 latitude bins between 0 and 15N would take the form [0,0,0,0,0,1] for extent factor=0, and [0.167,0.167, 0.167,0.167, 0.167,0.167] for extent factor=1. Injection ratios for intermediate values of the spread factor would be calculated by interpolation between these two end member cases.

1080



1081

1082

<u>Exp- Name</u>	<u>Specific description / Volcanic emission</u>	<u>Period</u>	<u>TIER</u>
PoEMS_OAT_med	SO ₂ Emission = medium, Inject shallow @medium-alt. Processes unperturbed.	Transient 1991-1995	1
PoEMS_OAT_P4h	SO ₂ Emission = medium, Inject shallow @medium-alt. Sedimentation rates doubled		2
PoEMS_OAT_P4l	SO ₂ Emission = medium, Inject shallow @medium-alt. Sedimentation rates halved		2
PoEMS_OAT_P5h	SO ₂ Emission = medium, Inject shallow @medium-alt. SO ₂ oxidation rates doubled		3
PoEMS_OAT_P5l	SO ₂ Emission = medium, Inject shallow @medium-alt. SO ₂ oxidation rates halved		3
PoEMS_OAT_P6h	SO ₂ Emission = medium, Inject shallow @medium-alt. Nucleation rates doubled		3
PoEMS_OAT_P6l	SO ₂ Emission = medium, Inject shallow @medium-alt. Nucleation rates halved		3
PoEMS_OAT_P7h	SO ₂ Emission = medium, Inject shallow @medium-alt. % SO ₂ as primary SO ₄ x2		3
PoEMS_OAT_P7l	SO ₂ Emission = medium, Inject shallow @medium-alt. % SO ₂ as primary SO ₄ x0.5		3
PoEMS_OAT_P8h	SO ₂ Emission = medium, Inject shallow @medium-alt. Coagulation rates doubled		2
PoEMS_OAT_P8l	SO ₂ Emission = medium, Inject shallow @medium-alt. Coagulation rates halved		2

1083

1084

1085

1086

1087

1088

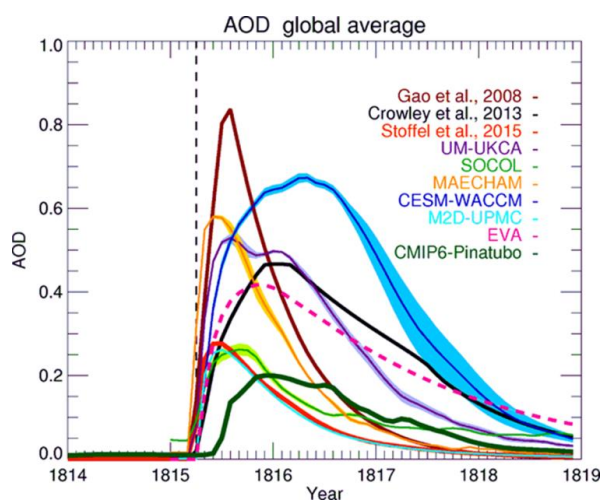
1089

Table 11: Overview of PoEMS One-At-a-Time” (OAT) test runs. Note that when imposing the parameter-scaling, the models should only enact the change in volcanically-enhanced air masses (where the total sulphur volume mixing ratio exceeds a threshold suitable for their model). Perturbing only the volcanically-enhanced air masses will ensure, pre-eruption conditions and tropospheric aerosol properties remains unchanged by the scalings.



1090 Figures

1091



1092

1093

1094

1095

1096

1097

1098

1099

1100

1101

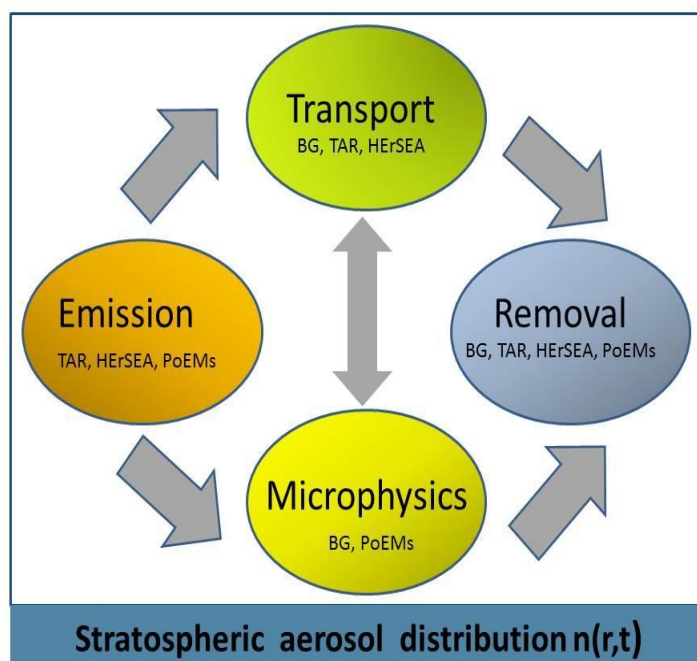
1102

1103

1104

Figure 1 Uncertainty in estimates of radiative forcing parameters for the 1815 eruption of Mt. Tambora: Global-average aerosol optical depth (AOD) in the visible band from an ensemble of simulations with chemistry–climate models forced with a 60 Tg SO₂ equatorial eruption, from the Easy Volcanic Aerosol (EVA, Toohy et al., 2016b) module with 56.2 Tg SO₂ equatorial eruptions (magenta thick dashed line), from Stoffel et al. (2015), from Crowley and Unterman (2013), and from Gao et al. (2008), aligned so that the eruption starts on April 1815). The estimate for the Pinatubo eruption as used in the CMIP6 historical experiment is also reported for comparison. The black triangle shows latitudinal position and timing of the eruption. Chemistry–climate models are CESM (WACCM) (Mills et al., 2016), MAECHAM5-HAM (Niemeier et al., 2009), SOCOL (Sheng et al., 2015a), UM-UKCA (Dhomse et al., 2014), and CAMB-UPMC-M2D (Bekki, 1995; Bekki et al., 1996). For models producing an ensemble of simulations, the line and shading are the ensemble mean and ensemble standard deviation respectively. Figure from Zanchettin et al. (2016).

1105

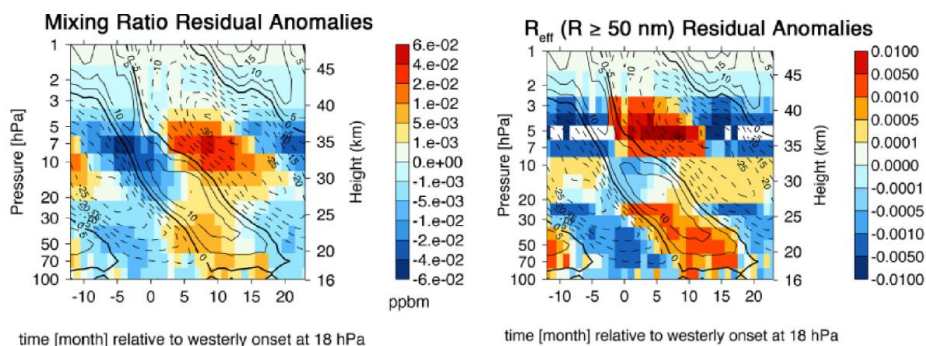


1106

1107

1108 **Figure 2** Schematic overview over the processes that influence the stratospheric aerosol size distribution. The related
1109 SSiRC experiments are listed below. BG stands for “BackGround”, TAR for “Transient Aerosol Record”, HErSEA
1110 for “Historical Eruption SO₂ Emission Assessment” and PoEMs for “Pinatubo Emulation in Multiple models”.

1111



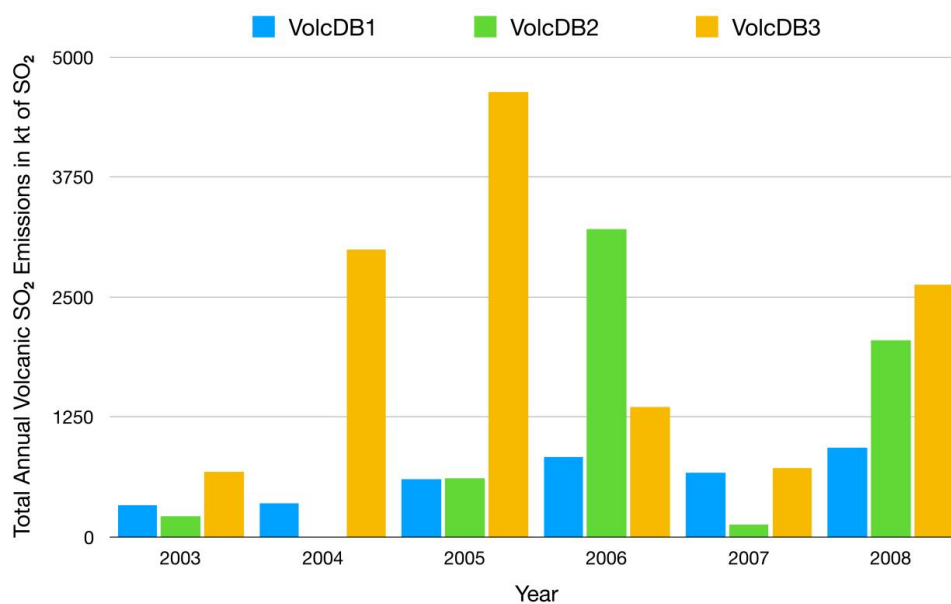
1112

1113 **Figure 3. (a) Composite of QBO-induced residual anomalies in the MAECHAM5-SAM2 modelled aerosol mass**
1114 **mixing ratio with respect to the time of onset of westerly zonal mean zonal wind at 18 hPa. Black contours denote the**
1115 **residual zonal wind. Dashed lines represent easterlies, contour interval is 5ms (b) same but for the modelled effective**
1116 **radius of aerosols with $R \geq 50$ nm. Figure from Hommel et al. (2015).**
1117



1118

1119



1120

1121

1122

1123

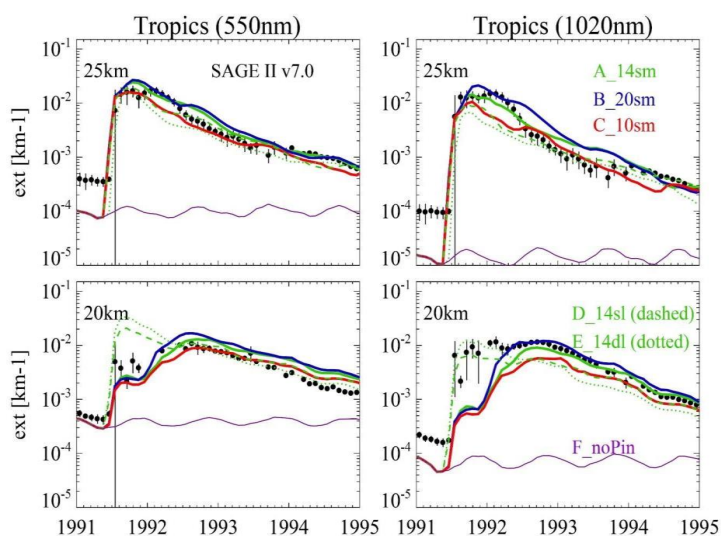
1124

Figure 4: Annual total volcanic sulfur dioxide (SO₂) emission from three different emission data sets between 2003 and 2008 to be used in the TIER1 MITAR experiments. VolcDB1 (Bingen et al., 2017) considers only stratospheric SO₂ emissions, VolcDB2 (Neely and Schmidt, 2016) and VolcDB3 (Carn et al., 2016) consider both tropospheric and stratospheric SO₂ emission.

1125

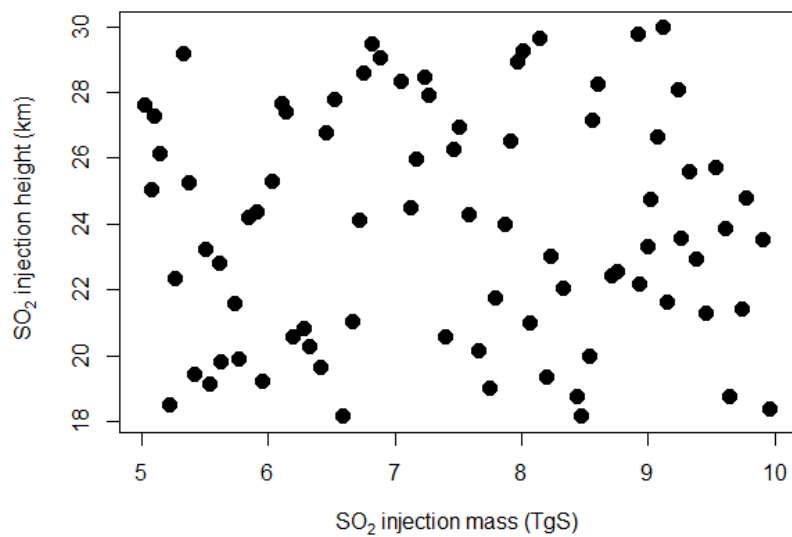


1126



1127

1128 **Figure 5:** Example results from interactive stratospheric aerosol simulations with the UM-UKCA model (Dhomse et
1129 al., 2014) of 5 different SO₂-injection-realizations of the 1991 Pinatubo eruption (see Table 3.3.1). The model tropical
1130 –mean extinction in the mid-visible (550nm) and near-infra-red (1020nm) is compared to that from SAGE-II
1131 measurements. Only 2 of the 5 injection realisations inject below 20km and the impact on the timing of the peak, and
1132 general evolution of the aerosol optical properties is apparent. In this model the growth to larger particle sizes and
1133 subsequent sedimentation to lower altitudes is able to explain certain signatures seen in the satellite data (see also
1134 Mann et al., 2015).



1135
1136
1137
1138
1139
1140

Figure 6 Illustration of the latin hypercube sampling method. Each dot represents the value used in one of the particular simulations with a perturbed parameter ensemble (PPE) with 50 members (realisations/integrations).



1141 **List of Abbreviations**

AEROCOM	Aerosol Comparisons between Observations and Models
AOD	Aerosol Optical Depth
AMOC	Atlantic Meridional Overturning Circulation
ASAP2006	Assessment of Stratospheric Aerosol properties (WMO, 2006)
AVHRR	Advanced Very High Resolution Radiometer
BDC	Brewer-Dobson Circulation
CALIOP	Cloud-Aerosol Lidar with Orthogonal Polarization
CALIPSO	Cloud-Aerosol Lidar and Infrared Pathfinder Satellite Observations
CATS	Cloud-Aerosol Transport System
CCM	Chemistry Climate Model
CCMVal	Chemistry-Climate Model Validation Activity
CCMI	Chemistry-Climate Model Initiative
CCN	Cloud Condensation Nuclei
CDN	Cloud Droplet Number Concentration
CDR	Cloud Droplet Radius
CMIP	Coupled Model Intercomparison Project
CMIP5	Coupled Model Intercomparison Project, phase 5
CMIP6	Coupled Model Intercomparison Project, phase 6
DJF	December-January-February
DWD	Deutscher Wetterdienst
ECHAM	European Center/HAMburg model, atmospheric GCM
EGU	European Geophysical Union
ECMWF	European Centre for Medium-Range Weather Forecasting
EESC	Equivalent Effective Stratospheric Chlorine
ENSO	El Niño Southern Oscillation
ENVISAT	Environmental Satellite
ERA-Interim	ECMWF Interim Re-Analysis
ERBE	Earth Radiation Budget Experiment
ESA	European Space Agency
ESM	Earth System Model
EVA	Easy Volcanic Aerosol
GCM	General Circulation Model
GHG	Green House Gases
GOMOS	Global Ozone Monitoring by Occultation of Stars
HALOE	Halogen Occultation Experiment
HD(CP)2	High definition clouds and precipitation for advancing climate prediction
ISA-MIP	Interactive Stratospheric Aerosol Model Intercomparison Project
ICON	ICOSahedral Nonhydrostatic
IPCC	Intergovernmental Panel on Climate Change
ISCCP	International Satellite Cloud Climatology Project (ISCCP)
ITCZ	Intertropical Convergence Zone
JAXA	Japanese Aerospace Exploration Agency



JJA	June-July-August
LAI	Leaf Area Index
LW	Longwave
LWP	Liquid Water Path
MiKIP	Mittelfristige Klimaprognosen
MIPAS	Michelson Interferometer for Passive Atmospheric Sounding
MODIS	Moderate Imaging Spectroradiometer
MPI-ESM	Earth System model of Max Planck Institute for Meteorology
NAO	North Atlantic Oscillation
NH	Northern hemisphere
OLR	Outgoing longwave radiation
OMI	Ozone Monitoring Instrument
OMPS	Ozone Mapping and Profiler Suite
OMPS-LP	Ozone Mapping and Profiler Suite–Limb Profiler
OPC	Optical Particle Counter
OSIRIS	Optical Spectrograph and InfraRed Imager System
PDF	Probability Density Function
POAM	Polar Ozone and Aerosol Measurement PSD
PSD	Particle Size Distribution
QBO	Quasi-biennial oscillation
RF	Radiative Forcing
RH	Relative Humidity
SAOD	Stratospheric Aerosol Optical Depth
SAGE	Stratospheric Aerosol and Gas Experiment
SAM	Southern Annular Mode
SCIAMACHY	Scanning Imaging Absorption Spectrometer for Atmospheric Chartography
SH	Southern Hemisphere
SPARC	Stratosphere-troposphere Processes And their Role in Climate
SSiRC	Stratospheric Sulfur and its Role in Climate
SST	Sea Surface Temperature
SW	Shortwave
TCS	Transient Climate Sensitivity
ToA	Top of the Atmosphere
TOMS	Total Ozone Mapping Spectrometer
TOVS	TIROS Operational Vertical Sounder
VEI	Volcanic Explosivity Index
VolMIP	Model Intercomparison Project on the climate response to Volcanic forcing

1142

1143